

Mauro César Sousa de Almeida

# APPLICATION OF MICELLEPLEXES OF PLURONIC L64-PEI-MIR-145 IN OSTEOSARCOMA THERAPY

Dissertação de Mestrado em Tecnologias do Medicamento, orientada pela Professora Doutora Ana Rita Figueiras, apresentada à Faculdade de Farmácia da Universidade de Coimbra

Setembro de 2017



UNIVERSIDADE DE COIMBRA



FFUC FACULDADE DE FARMÁCIA  
UNIVERSIDADE DE COIMBRA

Mauro César Sousa de Almeida

# Application of micelleplexes of Pluronic L64- PEI-miR-145 in osteosarcoma therapy

Dissertação de Mestrado em Tecnologias do Medicamento, orientada pela  
Professora Doutora Ana Rita Figueiras, apresentada à Faculdade de Farmácia da  
Universidade de Coimbra

Setembro de 2017

## Acknowledgements

À minha orientadora, Professora Doutora Ana Rita Figueiras, por toda a dedicação, apoio e pelas ideias e diferentes visões científicas. Obrigado pelo acompanhamento e pela disponibilidade constante.

À Mariana Magalhães, pela exigência, pelo apoio constante, pela atenção, pelo acolhimento e convívio e também pela paciência. Um grande obrigado por tudo!

Ao Professor Doutor Elisiário Silva e à Professora Doutora Carla Varela pela colaboração, pela disponibilidade, apoio, troca de ideias e dedicação.

A todos os elementos e funcionários do Laboratório de Tecnologia Farmacêutica agradeço a simpatia e ajuda prestada, principalmente à D. Gina pelo bom acolhimento e enorme disponibilidade.

Gostaria de reconhecer o Professor Doutor Francisco José de Baptista Veiga e a Professora Doutora Eugénia Pina pelo acolhimento e aconselhamento na Faculdade de Farmácia da Universidade de Coimbra.

Gostaria também de agradecer ao Laboratório de Oncobiologia e Hematologia por disponibilizar material e o equipamento de citometria de fluxo, imprescindíveis ao trabalho; à Mestre Joana Jorge, à Doutoranda Raquel Alves e à Doutora Ana Cristina Gonçalves pela grande ajuda, atenciosidade e pela partilha de conhecimento; ao Professor Doutor Alberto António Caria Canelas Pais, do Departamento de Química da FCTUC, pela ajuda, apoio e contribuições científicas para este trabalho; à Professora Doutora Maria José Moura, do Instituto Superior de Engenharia de Coimbra, pela ajuda e apoio prestado; ao grupo UCQ Farma por disponibilizar o espectrofotómetro ATR-FTIR; ao Doutor Nuno Ricardo pela ajuda e disponibilidade sempre demonstrada; ao laboratório de Ressonância Magnética Nuclear por disponibilizar o espectrómetro de RMN; ao Professor Doutor Rui Carvalho pela atenção e pelo tempo dispendido em prol do trabalho; ao Laboratório de Bio-imagem Celular de Alta Resolução da Faculdade de Medicina da Universidade de Coimbra por disponibilizar o microscópio de transmissão eletrónica; à Doutora Mónica Zuzarte pela disponibilidade de tempo para realização de imagens de TEM;

À Edna e à Maria Mendes pela amizade, que ao longo do tempo se foi construindo. Obrigado por me acolherem tão bem, pelo apoio, trocas de ideias, almoços, convívios e também, por vezes, pela paciência. Muito Obrigado.

Um agradecimento especial à Beatriz, que apesar de distante foi sempre o meu apoio diário. Obrigado pela tua motivação e pelo amor incondicional.

Por último e não menos importante, agradecer à minha família e amigos, em especial aos meus pais pelas oportunidades dadas para que eu crescesse a nível pessoal e profissional e pela confiança que sempre me transmitiram. Agradecimento também para a minha irmã Joana que com a sua inocência pura sempre demonstrou carinho, apoio e compreensão.

## **Resumo**

Encontrar novas terapias para tratar doenças como o cancro, é um dos focos da investigação em Ciências da Saúde. Na atualidade, as estratégias terapêuticas disponíveis para várias doenças têm, em muitos casos, limitações e efeitos colaterais indesejados, os quais mostram necessidade de novas terapias com uma eficácia maior. Neste sentido, a Medicina e todos os investigadores desta área, trabalham para obterem um tratamento seguro, menos invasivo, rápido e com uma grande percentagem de eficácia.

O osteossarcoma é o tipo mais comum de cancro que se desenvolve no osso e é normalmente encontrado no final de ossos longos, frequentemente ao redor do joelho. É correntemente tratado com uma estratégia combinada que consiste na remoção cirúrgica da lesão primária e quimioterapia com vários fármacos. A taxa de sobrevivência, nos últimos 30 anos, não aumentou para o osteossarcoma convencional de alto-grau e os fármacos utilizados são basicamente os mesmos desde os anos 70-80. Face a isto, devem ser encontradas terapias novas e alternativas que possam ser mais eficazes e mais seguras. Neste sentido torna-se essencial entender os principais mecanismos moleculares envolvidos na patogénese do osteossarcoma de forma a desenvolver novos agentes terapêuticos que tenham um alvo molecular específico para o tratamento de pacientes com osteossarcoma.

Perante tal facto, a terapia génica pode ser promissora na pesquisa e desenvolvimento de novas soluções terapêuticas para esta patologia. No entanto, a escolha e desenvolvimento de um vector que seja eficaz no transporte do material genético para a célula alvo é um dos desafios principais.

O objetivo deste trabalho foi conjugar o Pluronic L64 com uma polietilenimina (PEI) de baixo peso molecular, para formar uma poli(éster-amina), com capacidade de incorporar o miR-145 e, eficazmente, transportá-lo para o citoplasma de células de osteossarcoma.

**Palavras chave:** Osteosarcoma; miR-145; Pluronic L64; Polietilenimina; Poli(éster-amina); Micelleplexo

## **Abstract**

Find new therapies to treat diseases like cancer, it is one of the focus of Health Sciences research. Nowadays, the available therapeutic strategies for several diseases have in many cases limitations and undesired side effects, which show a need for new therapies with a higher efficacy. In this sense, the Medicine and all researchers working in this field work to have a treatment safer, less invasive, faster and with a large percentage of efficacy.

Osteosarcoma is the most common type of cancer that develops in bone and it is normally found at the end of long bones, frequently around the knee. It is currently treated with a combined approach consisting of the surgical removal of the primary lesion and chemotherapy with several drugs. The survival rate, in the last 30 years, for conventional high-grade Osteosarcoma has not increased and the drugs that are used are basically the same as those used since the years 70s-80s. Face to this, there must be new and alternative therapies that can be more effective and more safeness. Therefore, becomes essential understand the principal molecular mechanisms in Osteosarcoma pathogenesis in order to develop new therapeutic agents that have a specific molecular target for the treatment of patients with this pathology.

In this regard, gene therapy can be promising in the search and development of new therapeutic solutions for this pathology. However, the choice and development of a vector that can be effective in transporting the genetic material to the target cell is the main challenge.

The goal of this work was to conjugate the Pluronic L64 with a low molecular weight polyethyleneimine (PEI), to form a poly(ester amine), that been able to incorporate miR-145 and, efficiently, transport it to the cytoplasm of osteosarcoma cells.

**Key-words:** Osteosarcoma; miR-145; Pluronic L64; Polyethyleneimine; Poly(ester amine); Micelleplex

## Contents

<b>I. Introduction</b> .....	1
1.1 Osteosarcoma .....	1
1.1.1 Pathophysiology .....	1
1.1.2 Predisposing conditions and genetic alterations .....	3
1.1.2.1 Germline mutation disorders .....	3
1.1.2.2 miRNAs .....	4
1.1.2.2.1 miRNA-145 .....	4
1.2 Gene therapy .....	5
1.2.1 Viral and non-viral vectors .....	6
.....	7
1.2.1.1 Cationic Polymers.....	7
1.2.1.1.1 Polyethyleneimine (PEI) .....	8
1.2.1.2 Poloxamers.....	10
1.2.1.2.1 Pluronic (Poloxamer) L64.....	12
1.2.1.3 Polymeric micelles .....	13
1.2.1.3.1 Micelleplexes .....	17
1.2.1.3.1.1 Micelleplex preparation .....	18
1.2.3.1.1.2 Challenges to micelleplex delivery .....	18
1.3 Aims .....	20
<b>2 Material and Methods</b> .....	21
2.1 Materials.....	21
2.2 Synthesis of Pluronic L64 Diacrylate .....	21
2.3 Synthesis of cationic PEA complexes (L64 diacrylate + PEI).....	22
2.4 Preparation of PEA micelles .....	23
2.5 Micelleplexes preparation .....	23
2.6 Conjugation of micelleplexes with Rhodamine-B.....	24
2.7 Complexes characterization.....	24

2.7.1 Particle size, zeta potential, and molecular weight .....	24
2.7.2 <sup>1</sup> H-NMR spectroscopy .....	25
2.7.3 Fourier transform-infrared spectroscopy (FTIR) .....	25
2.7.4 Transmission Electron Microscopy .....	25
2.8 Agarose gel electrophoresis assay .....	25
2.8.1 Quantification method .....	26
2.9 Cell culture.....	26
2.9.1 Binding and uptake assay.....	26
2.9.2 Cell death assessment .....	27
2.9.2.1 Flow cytometry .....	27
2.9.3 Cell viability assay .....	28
2.10 Statistical analysis.....	29
<b>3 Results and discussion .....</b>	<b>30</b>
3.1 Synthesis of Pluronic L64 Diacrylate .....	30
3.2 Synthesis of cationic PEA complexes (PEI+L64 diacrylate) .....	31
3.3 Complexes characterization.....	33
3.3.1 PEA micelles .....	33
3.3.2 Micelleplexes optimization .....	34
3.3.2.1 Encapsulation efficiency .....	36
3.3.3 Micelleplexes with miR-145 mimic .....	37
3.3.3.1 Encapsulation efficiency .....	38
.....	39
3.3.4 Morphology characterization.....	39
3.4 Binding and uptake assay .....	40
3.5 Cell death assessment.....	41
3.5.1 Cell viability.....	41
3.5.2 Flow cytometry.....	43
.....	45

<b>4. Conclusion and future perspectives .....</b>	<b>48</b>
<b>5. References .....</b>	<b>49</b>

## List of abbreviations and acronyms

**ABC** Amphiphilic block copolymer

**AV** Annexin-V

**BPEI** Branched PEI

**CIN** Chromosomal instability

**CMC** Critical micelle concentration

**CMT** Critical micelle temperature

**CO<sub>2</sub>** Carbon dioxide

**DLS** Dynamic light scattering

**DMEM-HG** Dulbecco's modified Eagle medium – high glucose

**DNA** Deoxyribonucleic acid

**EO** Ethylene oxide

**EPA** Environmental protection agency

**EPR** Enhanced permeability retention

**FBS** Fetal bovine serum

**FDA** Food and drug administration

**FTIR** Fourier transform infrared spectroscopy

**<sup>1</sup>H-NMR** Proton Nuclear magnetic resonance

**HBS** HEPES-buffered saline

**HLB** Hydrophilic-lipophilic balance

**LFS** Li-Fraumeni syndrome

**LPEI** Linear PEI

**miRNA/miR** microRNA

**MMP16** Metalloproteinase 16

**mRNA** Messenger RNA

**MW** Molecular weight

**MWCO** Molecular weight cut-off

**NT** Non-targeted

**OS** Osteosarcoma

**PAMAM** Polyamide Amine

**PBS** Phosphate buffered saline

**PDI** Polydispersion index

**PEA** Poly(ester amine)

**PEI** Polyethyleneimine

**PEO** Polyethylene oxide

**PI** Propidium iodide

**PLL** Poly-L-lysine

**PO** Propylene oxide

**PPO** Polypropylene oxide

**pRb** Retinoblastoma protein

**RES** Reticuloendothelial system

**RFU** Relative fluorescence units

**RITC** Rhodamine B isothiocyanate

**RNA** Ribonucleic acid

**ROCK1** Rho-associated protein kinase I

**SD** Standard deviation

**siRNA** small-interfering RNA

**TBE** Tris/Borate/EDTA

**TEM** Transmission electron microscopy

**UV/VIS** Ultraviolet/Visible Spectrophotometry

**VEGF** Vascular endothelial growth factor

## **List of scientific publications**

ALMEIDA, Mauro *et al.* - Poloxamers, poloxamines and polymeric micelles: Definition, structure and therapeutic applications in cancer. **Journal of Polymer Research**. (*Under review*)

## Index of figures

<b>Figure 1</b> - Different types of carriers employed in gene delivery. Adapted (Jafari et al., 2012) .....	7
<b>Figure 2</b> - Schematic representation of proton sponge effect of PEI (Jin et al., 2014). .....	10
<b>Figure 3</b> - Pluronic L64 block copolymer contain two hydrophilic EO blocks and a hydrophobic PO block. Adapted (Kabanov, Zhu e Alakhov, 2005).....	13
<b>Figure 4</b> - Polymeric micelles as (a) drug and (b) nucleic acid (micelleplex) delivery systems. Adapted (Wang et al., 2016). .....	16
<b>Figure 5</b> - Stages of intracellular miRNA delivery. (A) Micelleplex interaction with the cell membrane results in the internalisation of the micelleplex by macropinocytosis, phagocytosis, or receptor-mediated endocytosis (caveolae and clathrin). (B) Formation of the early endosome (i). Micelleplexes trapped in the endosome are digested in the late endosome and/or lysosome (ii) and removed from the cell by exocytosis (iii). (C) Alternatively, if the micelleplex induces endosomal escape (i), it travels through the cytoplasm, where the polymer is gradually degraded by cytoplasmic or intracellular enzymes (ii). miRNA binds to RNA-induced silencing complex (RISC) (iii) and binds to mRNA target causing your cleavage or translational repression (iv). (D) Also, exists the possibility of the miRNA interacts with different mRNA targets, by alternative targeting (i) or be degraded (ii). Adapted (Aied et al., 2013; Tomaselli et al., 2013; Yin et al., 2014).....	19
<b>Figure 6</b> - Parallel synthesis of cationic PEA complexes in a Radleys carrousel. ....	23
<b>Figure 7</b> - FTIR spectra of Pluronic L64 and Pluronic L64 diacrylate. The numbers 1 and 2 represent functional groups (confront scheme 1). .....	30
<b>Figure 8</b> - <sup>1</sup> H-NMR spectra of Pluronic L64 (a) and Pluronic L64 diacrylate (b). .....	31
<b>Figure 9</b> - <sup>1</sup> H-NMR spectra of PEI (a), PEA 1(b), PEA 2 (c) and PEA 3 (d). .....	32
<b>Figure 10</b> - FTIR spectra of Pluronic L64, L64 diacrylate, PEI, PEA 1, PEA 2 and PEA 3. The number 3 represents a functional group (confront scheme 1). .....	33
<b>Figure 11</b> - DLS data of micelleplexes for different PEA and different N/P ratios, in terms of (a) particle size, (b) PDI and (c) zeta potential. (*p < 0,05) .....	36
<b>Figure 12</b> - Representation of an agarose gel retardation assay with the different PEAs and different N/P ratios.....	37
<b>Figure 13</b> - DLS data of micelleplexes with miR-145 mimic for PEA 2 at ratios 5/1 and 10/1 (N/P), in terms of (a) particle size, (b) PDI and (c) zeta potential.....	38
<b>Figure 14</b> - Representation of an agarose gel retardation assay with miR-145 mimic and two N/P ratios 5/1 and 10/1.....	39

**Figure 15** - TEM images of PEA 2 micelles (a), and of micelleplexes with ratio 10/1 (N/P) at a concentration of 50nM of miR-145 mimic (b).....40

**Figure 16** - Results from binding(a), and internalization (b), of micelleplexes at different ratios and concentrations, expressed in relative fluorescence units (RFU). The ratios 5/1 and 10/1 are related to N/P ratio and 10nM and 50nM refer the concentration of miR-145 mimic. (\*p < 0.05).....41

**Figure 17** - Cell viability of different polymers, Pluronic L64 and PEI (a), and PEA 1, 2 and 3 (b) at concentrations of 5, 10, 20 and 40µg/mL. (\*p < 0.05) .....42

**Figure 18** - Cell viability of micelleplexes with different ratios and concentrations at 24hours (a) and 48hours (b) after transfection. The ratios 5/1 and 10/1 are associated with N/P ratio and the expression “NT” refers to the use of miR non-target. 10nM and 50nM refers the concentration of miR-145 mimic or, when applicable, the miR non-target. (\*p < 0.05).....43

**Figure 19** - Flow cytometry results of all conditions (a), and images of flow cytometry of control (b), ratio 10/1 50nM non-targeted, (c) and ratio 10/1 50nM (d). The 5/1 and 10/1 are associated with N/P ratio and the expression “non-targeted” refers to the use of miR non-target. 10nM and 50nM refer the concentration of miR-145 mimic or, when applicable, the miR non-target. The different quadrants in flow cytometry images (b), (c) and (d) means: lower left quadrant – living cells; lower right quadrant – necrotic cells; upper left quadrant – apoptotic cells; upper right quadrant – late apoptotic cells/ secondary necrotic cells.....45

**Figure 20** - Optical microscopy images of different conditions tested. Non-treated cells, which represents a normal cell (a), 10/1 (N/P) with 50nM of miR-145 mimic, representing an apoptotic cell (b) and same condition, 10/1 (N/P) 50nM of miR-145 mimic, representing a necrotic cell (c). The images were taken at a final magnification of 1000x.....47

## Index of tables

<b>Table 1</b> - Classification and sub-types of OS in function of grade (Adapted <sup>6-8,10</sup> ).....	2
<b>Table 2</b> - Advantages and disadvantages of common natural and synthetic cationic polymers in gene delivery applications. Adapted <sup>26</sup> .....	8
<b>Table 3</b> - Physicochemical characteristics of Pluronic® and poloxamer block copolymers. Adapted <sup>35,36,39,45</sup> .....	12
<b>Table 4</b> - Characteristics of PEA.....	31
<b>Table 5</b> - Characteristics of developed PEA, in terms of particle size, zeta potential and molecular weight.....	34
<b>Table 6</b> - Data from encapsulation efficiency of different PEAs for ratio 1/1 (N/P) .....	37

## **Index of schemes**

<b>Scheme I</b> - Synthesis of Pluronic L64-PEI (PEA) copolymers. The numbers 1,2 and 3 represent functional groups. ....	23
---	----

# **I. Introduction**

## **I.1 Osteosarcoma**

Osteosarcoma (OS), the most common malignant tumor of bone in childhood and adolescent, is a very aggressive neoplasm characterized by a high level of malignancy, relapse, and metastasis, being characterized by malignant osteoid production and osteoblastic differentiation (Li *et al.*, 2014). This pathology has an annual incidence rate of 4.4 cases per million (Miao *et al.*, 2013).

The treatment of OS consists in the surgical removal of the primary lesion and systemic pre- and postoperative multidrug chemotherapy, that includes doxorubicin, cisplatin, high-dose methotrexate and/or ifosfamide and/or etoposide (Serra e Hattinger, 2016). OS patients have a poor prognosis with an overall 5-years survival time, presenting a survival rate between 55%–68%, which has not increased in the last 30 years (Fan *et al.*, 2012; Serra e Hattinger, 2016).

Some efforts have been exerted during the past decades, but the prognosis of advanced OS and the molecular mechanisms involved in the tumor development still remains poor, which can be attributed to the complex structure and numerous genomic rearrangements of bone cancer cells (Martin, Squire e Zielenska, 2012). Defects in genes that are involved in DNA repair and tumor suppressor pathways also might contribute to the pathogenesis of OS (Miao *et al.*, 2013). Thereby, the principal cause of this genomic instability in OS is the chromosomal instability (CIN), which is characterized by the elevated rate of gain or loss of entire chromosomes or sections of chromosomes (Martin, Squire e Zielenska, 2012).

### **I.1.1 Pathophysiology**

OS can be developed by different ways in several parts of the body and it can be classified, according to the World Health Organization, as primary, which is sub-typed as intramedullary/central and surface osteosarcomas, and as secondary, which is associated with other factors like Paget's disease (Fletcher, C. D.M., Bridge, J.A., Hogendoorn, P., Mertens, 2013; Kundu, 2014). Based on the histological appearance and the capacity of tumor growth, the different subtypes can be grouped into three categories, namely high-grade,

intermediate-grade, and low-grade (Lindsey, Markel e Kleinerman, 2016). Thereby, in accord with a wide range of research studies, the most frequent type of osteosarcoma that occurs are the high-grade subtypes, osteoblastic, chondroblastic, and fibroblastic variants (American Cancer Society, 2016; Durfee, Mohammed e Luu, 2016; Kundu, 2014; Lindsey, Markel e Kleinerman, 2016; Martin, Squire e Zielenska, 2012; Serra e Hattinger, 2016). (Table I)

As mentioned before, OS develops mainly in children and adolescents usually at the end of long bones, mainly in the knee, and these findings suggest a relationship between the hormonal changes of puberty and/or physiologic bone growth and the pathogenesis of OS (Durfee, Mohammed e Luu, 2016; Miao *et al.*, 2013). The OS can also occur at any age and in any bone, however, it affects, mostly, the bones around the knee, either in the distal femur or the proximal tibia, and the proximal humerus (American Cancer Society, 2016; Durfee, Mohammed e Luu, 2016; Lindsey, Markel e Kleinerman, 2016; Serra e Hattinger, 2016).

Table I - Classification and sub-types of OS in function of grade (Adapted (American Cancer Society, 2016; Fletcher, C. D.M., Bridge, J.A., Hogendoorn, P., Mertens, 2013; Kundu, 2014; Lindsey, Markel e Kleinerman, 2016))

		High-grade	Intermediate-grade	Low-grade
<b>Primary</b>	Intramedullary/ Central	Osteoblastic (50%)		Intramedullary or intraosseous well differentiated
		Chondroblastic (25%)		
		Fibroblastic (25%)		
		Mixed		
		Small cell		
		Telangiectatic		
	Surface	Surface(juxtacortical)	Periosteal (juxtacortical)	Parosteal (juxtacortical)
<b>Secondary</b>		Pagetoid		
		Extra-skeletal		
		Post-radiation		

## **1.1.2 Predisposing conditions and genetic alterations**

There are several difficulties in understanding the molecular mechanisms involved in OS development due to the complex structure and numerous genomic rearrangements of bone cancer cells (Miao *et al.*, 2013). The majority of the cases are sporadic without a known environmental or genetic cause, however, it is known that OS cells tend to exhibit extreme genetic pleomorphism, which is the most likely reason for their strong chemotherapy resistance (Fletcher, C. D.M., Bridge, J.A., Hogendoorn, P., Mertens, 2013; Miao *et al.*, 2013).

Thus, the principal genetic alterations in OS are associated with CIN, being that the usual genetic alterations are losses of portions of chromosomes 3q, 6q, 9, 10, 13, 17p, and 18q and gains of portions of chromosomes 1p, 1q, 6p, 8q, and 17p (Martin, Squire e Zielenska, 2012).

### **1.1.2.1 Germline mutation disorders**

It was observed a predisposition for developing OS in a few germline mutation disorders including hereditary retinoblastoma, Rothmund–Thomson syndrome, Li Fraumeni syndrome, and Bloom syndrome, among others (Durfee, Mohammed e Luu, 2016; Kundu, 2014; Lindsey, Markel e Kleinerman, 2016; Miao *et al.*, 2013). Retinoblastoma is a pathology characterized by germline mutation in RB1 gene, and a person with this condition has about 1000-fold increased risk of OS (Durfee, Mohammed e Luu, 2016; Kundu, 2014). The RB1 gene codifies to the pRb (retinoblastoma protein) that, when unexpressed, induces a dysregulation of the cell cycle (Durfee, Mohammed e Luu, 2016). Li–Fraumeni syndrome (LFS), associated with a germline mutation in TP53 gene, is a rare condition but the main predisposition to pediatric sarcomas (Durfee, Mohammed e Luu, 2016; Lindsey, Markel e Kleinerman, 2016). However, mutations in TP53 gene do not occur only in this syndrome, being common in other types of cancer. (Durfee, Mohammed e Luu, 2016; Kundu, 2014; Martin, Squire e Zielenska, 2012). Others alterations in genes are also associated with increased risk of OS, among them there exists the genes CDK4, PRIMI, CDKN2A, MDM2, RECQL2 (Werner syndrome), RECQL3 (Bloom syndrome) and RECQL4 (Rothmund-Thomson syndrome) (Durfee, Mohammed e Luu, 2016; Kundu, 2014; Lindsey, Markel e Kleinerman, 2016; Martin, Squire e Zielenska, 2012; Miao *et al.*, 2013; Serra e Hattinger, 2016).

### **1.1.2.2 miRNAs**

The knowledge of the mechanism of action of miRNAs in OS is extremely important, because it is known that, in this pathology, several miRNAs like miR-9, miR-99a, miR-195, miR-148a, miR-181a, miR-143, miR-145, miR-335 and miR-539 are dysregulated and may act as potential biomarkers in the diagnosis, treatment and prognosis of OS (Hu *et al.*, 2012).

MicroRNAs (miRNAs) are the most-studied noncoding RNAs, they are small RNA molecules which can interfere with the expression of several genes and act as gene regulators. They are short nucleic acids with 18–25 nucleotides, a single strand, and a high-degree conservation of structure and function in animals (Miao *et al.*, 2013). They can regulate gene expression once they perform an imperfect base pairing with sequences on the 3' untranslated regions (UTR) of the target messenger RNAs (mRNAs), inhibiting their expression by inducing the repressing of their translation (Fan *et al.*, 2012). Over 2500 miRNAs have been identified in the human genome, which are thought to regulate up to 60% of protein-coding genes at the translational level (Catalanotto, Cogoni e Zardo, 2016; Cui, Wang e Chen, 2014). Because of their ubiquitous role, they emerged as fundamental components of nearly every biological process, like cell proliferation, migration, differentiation and their dysregulation has been related to various pathological disorders, including several types of cancer (Catalanotto, Cogoni e Zardo, 2016). Face to this it can be inferred that microRNAs can act as oncogenes or tumor suppressors.

#### **1.1.2.2.1 miRNA-145**

Downregulation of miR-145 expression is associated with a worse prognosis for many cancers, indicating that it may serve as a potential cancer biomarker and an attractive target for cancer therapy.

Recently, miR-145 was associated with many types of cancer, regulating various cellular processes, such as the cell cycle, proliferation, apoptosis, and invasion, by targeting multiple oncogenes. It is an important member of the family of microRNAs and it is expressed in several types of tumors like lung, breast, ovary, prostate, colon, including also the OS. (Cui, Wang e Chen, 2014).

MiR-145 is located in human on chromosome 5 (5q32-33) and is suggested to be co-transcribed with miR-143 (Das e Pillai, 2015). The biogenesis of miRNAs occurs through a process requiring both a nuclear and a cytoplasmic phase (Catalanotto, Cogoni e Zardo, 2016;

Cui, Wang e Chen, 2014; Das e Pillai, 2015). In a final phase, in the cytoplasm, one strand of the mature miRNA bonds an Argonaute protein to form a RNA-induced silencing complex (RISC), which target the complementary sequence of mRNAs, whereas the other strand of the mature miRNA is usually degraded. Moreover, this miRNA targeting complementary can be perfect or imperfect, resulting in mRNA cleavage or translational repression, respectively (Winter *et al.*, 2009). A single miRNA can potentially target to several mRNAs (Catalanotto, Cogoni e Zardo, 2016; Cui, Wang e Chen, 2014; Winter *et al.*, 2009).

The miRNAs exercise a significant role in important pathways, like signal-transduction and oncogenic, in order to maintain normal cell function (Miao *et al.*, 2013). It was demonstrated that miR-145 has specific targets in OS cells, like the vascular endothelial growth factor (VEGF), the metalloproteinase 16 (MMP16), the Friend leukemia virus integration 1 (FLI-1) and the Rho-associated coiled-coil kinase (ROCK1)(Chen *et al.*, 2015; Fan *et al.*, 2012; Li *et al.*, 2014; Wan *et al.*, 2014; Wu *et al.*, 2016). In this sense, understanding the specific targets of miRNAs, like miR-145, and how they affect the specific oncogenic pathways related to OS, becomes fundamental to a successful application of miRNAs as therapeutic agents.

## **1.2 Gene therapy**

Gene therapy contributed to the appearance of new therapeutic approaches to treat genetic disorders, this because it consists in, permanently or transiently, replace genetic defects with exogenous nucleic acids (Kim *et al.*, 2015). Gene therapy is capable of suppressing cancerous cells, mitigate cardiovascular diseases, correct neurological disorders but also, in the case of infection, the removal of infectious pathogens (Collins e Thrasher, 2015; Jafarlou *et al.*, 2016).

However, associated with gene therapy exists the necessity of having systems to transport the genetic material, in order to avoid their degradation by nucleases, well as to promote an efficient delivery into the target cells/tissue. Nano-sized systems including liposomes, water-soluble polymeric carriers, nano-spheres and polymeric micelles are being used to deliver nucleic acids, but also drugs, proteins and other therapeutic agents, which contributes for a considerable publication of articles in the last decade (Yokoyama, 2014).

The goal of this therapeutic approach is to develop safe systems that can efficiently deliver nucleic acids. Examples of nucleic acids, that are used in gene therapy, include DNA

(oligonucleotides, plasmid, viruses, artificial chromosomes, and bacteria) and RNA (oligonucleotides, ribozymes, siRNA, miRNA, mRNA, and viruses) (Jafari *et al.*, 2012).

### 1.2.1 Viral and non-viral vectors

The delivery of nucleic acids into a target cell can be performed through the use of viral or non-viral vectors. The viral vectors, like adenovirus and lentivirus, are highly effective but present some disadvantages, like the possibility to be immunogenic and/or tumorigenic, meanwhile the non-viral vectors, which includes physical and chemical systems, have more safety and less cost-effectiveness, but lower efficiency (Collins e Thrasher, 2015; Jafari *et al.*, 2012; Jafarlou *et al.*, 2016; Kim *et al.*, 2015; Nayerossadat, Ali e Maedeh, 2012). In the non-viral vectors, the physical systems englobe hydrodynamic delivery, ultrasound, electroporation, magnetofection, gene gun or photodynamic therapy where a physical force (mechanical, magnetic, ultrasonic, electrical field or laser-based energy) allows the possibility of penetrating the target cells membrane, transiently (Jafari *et al.*, 2012; Jin *et al.*, 2014; Nayerossadat, Ali e Maedeh, 2012). Also in non-viral vectors, exists the possibility of carrying the genetic material with chemical systems, like liposomes and polymeric cationic vectors, natural and/or synthetic (Guo e Huang, 2013; Kim *et al.*, 2015; Nayerossadat, Ali e Maedeh, 2012).

The naked molecules of DNA/RNA, except for direct penetration of the cell membrane, are not able to transfect a cell, since they are degraded by enzymes, nucleases, present in the blood flow, being necessary to encapsulate the nucleic acids in a carrier system to protect them (Keles *et al.*, 2016). The vector needs to establish electrostatic interactions with the negatively charged DNA/RNA molecule, transport it to a specific target, enter in the cell cytoplasm or nucleus and disintegrated to release the nucleic acids (Jafari *et al.*, 2012; Keles *et al.*, 2016). The choice and optimization of a vector become the challenge and the vector/carrier should be capable of increasing the transfection efficiency, but being always safe, in other words, non-immunogenic, nontoxic and noncarcinogenic (Collins e Thrasher, 2015; Guo e Huang, 2013; Keles *et al.*, 2016).

The transference of nucleic acids mediated by viral vectors is called transduction, and can involve the retroviruses (e.g. MLV, HIV), adenoviruses, the non-pathogenic human parvovirus adeno-associated virus (AAV), lentiviruses, herpes simplex viruses and hybrid viruses (Collins e Thrasher, 2015; Jafarlou *et al.*, 2016; Ji, Sun e Su, 2017). In order to turn safer the viral vectors, deletions of few areas of their genomes have been done, however,

these vectors still induce inflammatory responses and are limited in transgenic capacity size (Nayerossadat, Ali e Maedeh, 2012).

The transfection is the expression given to the gene therapy guided by non-viral vectors, which usually involves cationic lipids or polymers (Guo e Huang, 2013). This is the ideal method, in terms of defined composition and manufacturing reproducibility (Collins e Thrasher, 2015). Based on the type of the nanocarrier, it can be obtained several structures with different properties and capacities to incorporate and to transport the nucleic acids to the target cells. The conjugation of the nucleic acids with different vectors, allows the formation of various complexes, such as lipoplexes, complexes formed by lipid vectors, usually cationic, polyplexes, composed by polymeric vectors, commonly cationic too, and also nanoplexes, where polymers or other molecules, like atelocollagen, are used in conjugation with nucleic acids to form nanoparticles (Jafari *et al.*, 2012) (Figure 1).

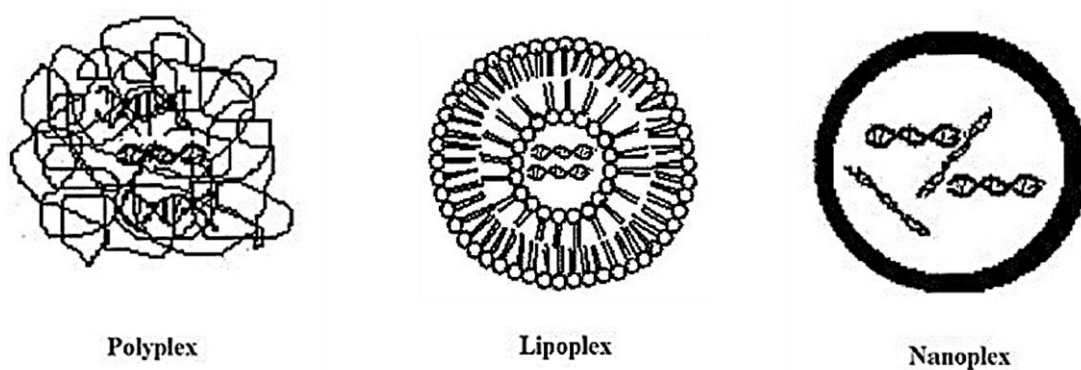


Figure 1 - Different types of carriers employed in gene delivery. Adapted (Jafari *et al.*, 2012)

### 1.2.1.1 Cationic Polymers

Different cationic polymers have been studied and synthesized, in order to be applied in gene therapy strategies, which can be attributed to their advantages, such as biodegradability, nontoxicity, and capability to promote an efficient cellular uptake (Jafari *et al.*, 2012). Until now, it has been used a large variety of polymers like the polypeptide poly-L-lysine (PLL); the synthetics polyethyleneimine (PEI), the poly-amidoamine (PAMAM) dendrimers and the natural chitosan and cyclodextrins, which are described in Table 2 (Jin *et al.*, 2014; Keles *et al.*, 2016; Kim *et al.*, 2015).

The use of cationic polymers with biodegradability properties is required in order to minimize the accumulation of these polymers in tissues (Keles *et al.*, 2016). The intrinsic physicochemical characteristics of polymeric particles such as particle size, surface charge,

chemical functional groups and N/P ratio have a direct influence on the encapsulation of genetic material, on the tumor targeting, on the cellular uptake and on the escape from the lysosome (Jin *et al.*, 2014; Kim *et al.*, 2015). Thus, it is possible to define a relationship between the length of the polymer with its toxicity and its capacity to perform an efficient transfection (Nayerossadat, Ali e Maedeh, 2012). Polymers with bigger molecular weight also have a higher net positive charge, improving their ability to bind DNA/RNA molecules, subsequently leading to more stable complexes (Keles *et al.*, 2016; Nayerossadat, Ali e Maedeh, 2012). However, this increase translates in higher toxicity (Keles *et al.*, 2016; Nayerossadat, Ali e Maedeh, 2012).

Table 2 - Advantages and disadvantages of common natural and synthetic cationic polymers in gene delivery applications. Adapted (Keles *et al.*, 2016)

Polymer	Nature	Advantages	Disadvantages
Poly-L-lysine	Natural	Biodegradable peptide-based structure: similar to protamine and other amphiphilic peptides	Poor transfection efficiency
Chitosan		Biodegradable and digestible	Poor transfection efficiency Poor solubility in aqueous solutions
Cyclodextrin		Excellent biocompatibility and biodegradability	Difficulty in processing
Polyethyleneimine	Synthetic	High positive charge density: increased loading capacity and transfection efficiency	High toxicity
Poly-amidoamine dendrimers		Low toxicity, high transfection efficiency, and ease of manufacturing	Poor biodegradability

### 1.2.1.1.1 Polyethyleneimine (PEI)

PEI is a synthetic polymer composed of repeating units of amine groups and two aliphatic carbons, that are commercially available under linear or branched-PEI, with molecular weights between some hundred Daltons to about 1000 kDa (Höbel e Aigner, 2013; Lungu *et al.*, 2016). The branched PEI (BPEI) has primary, secondary, and tertiary amino groups and it is liquid at room temperature, whereas the linear PEI (LPEI) only possesses secondary and primary amino groups and it is solid at the same temperature (Lungu *et al.*, 2016). PEI has been

utilized in the last decades in various industrial processes such as water purification, paper production, a flocculating agent, while its application in cellular transfection was only described in 1995 (Höbel e Aigner, 2013).

PEI has been extremely investigated, in the last 20 years, because of its nucleic acid condensation capacity, thanks to its amino groups, but also to its unique buffering capacity in endosomes called proton sponge effect, that facilitates the release of the nucleic acids to the cytoplasm through osmotic swelling and burst of endosomes (Jin *et al.*, 2014; Mien-Chie Hung, Leaf Huang, 2014). The proton sponge effect can be divided into several steps, firstly protons enter in the endosomes causing acidification, secondly there is an accumulation of protons through the endosomal ATPase with an influx of chloride anions, next the presence of PEI leads to an increase in the ionic concentration causing water entry and subsequent swelling of the endosome, followed by the “umbrella” effect associated with polymer expansion due to internal charge repulsion. All these processes will lead to rupture of the endosomal membrane and release of the nucleic acids into the cytoplasm (Jin *et al.*, 2014; Keles *et al.*, 2016; Mien-Chie Hung, Leaf Huang, 2014)(Figure 2).

The conjugation of PEI with nucleic acids leads to the formation of a polyplex (Wang *et al.*, 2016). The transfection efficiency and biocompatibility of PEI-based polyplexes are determined especially by the structure and molecular weight of the polymer (Höbel e Aigner, 2013). Branched PEI presents a better conjugation with nucleic acids and a better endosomal escape capacity. Also, PEI with high molecular weight, more than 20KDa, is more efficient but is also more cytotoxic than PEI with low molecular weight (Mien-Chie Hung, Leaf Huang, 2014). Another problem associated with the *in vivo* transfection of PEI particles is the tendency to aggregate with blood components (Jin *et al.*, 2014). In fact, it is a challenge to prepare PEI-based vectors with low cytotoxicity and high transfection efficiency. All the advantages of PEI, like high charge density and proton-sponge effect, and disadvantages, like cytotoxicity and opsonization, made necessary the emergence of alterations on the physicochemical properties, like conjugation with other polymers and lipids, and/or its conjugation with ligands for a targeted delivery (Höbel e Aigner, 2013; Lungu *et al.*, 2016; Mien-Chie Hung, Leaf Huang, 2014; Wang *et al.*, 2016).

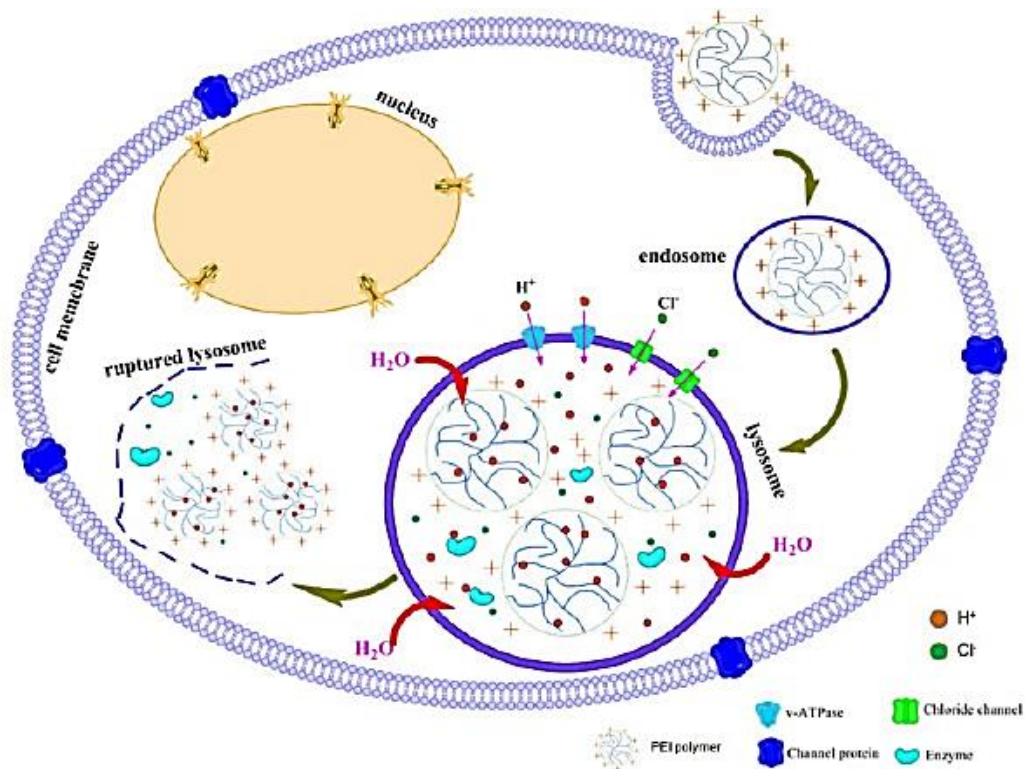


Figure 2 - Schematic representation of proton sponge effect of PEI (Jin et al., 2014).

### 1.2.1.2 Poloxamers

The use of amphiphilic block copolymers (ABCs) in pharmaceutical sciences has a long history and a rapid development (Xiong et al., 2011). The chemical flexibility of the ABCs makes possible the production of micelles with an almost infinite number of sophisticated structures, giving the possibility to refine and to optimize the physicochemical properties of these systems in order to incorporate a drug or a DNA/RNA molecule, acting as vectors, taking into account the pathophysiology of the disease (Xiong et al., 2011; Yokoyama, 2014).

Poloxamers are an example of block copolymers, available under the trade name of Pluronic® (BASF), Lutrol® (BASF), Kolliphor® (BASF), Synperonic® (Croda), and Antarox® (Rhodia) (Jung et al., 2013; Tavano et al., 2016; Torcello-Gómez et al., 2014).

They are formed by two hydrophilic PEO blocks at each end, which are linked to a hydrophobic PPO block that is in the middle of the chain (Jung et al., 2013). Poloxamers are synthesized by the sequential addition of PO and EO monomers in the presence of an alkaline catalyst, such as sodium or potassium hydroxide (Kabanov, Batrakova e Alakhov, 2002). Different poloxamers can be produced by varying the number of hydrophilic EO and hydrophobic PO units, which are characterized by a distinct hydrophilic-lipophilic balance (HLB) (Fan et al., 2012; Kabanov, Batrakova e Alakhov, 2002) (Table 1). Also, there exists an inverted substructure composed by PPO-PEO-PPO sequence, known as reverse poloxamers

and they are commercially available by the trade name Pluronic<sup>®</sup> R and Antarox<sup>®</sup> R, being used as wetting and defoaming agents in industrial processes (D'Errico, Paduano e Khan, 2004). The hydrophobicity of PPO at temperatures exceeding the cloud point (>15 °C) and the high hydrophilicity of PEO in temperatures between the 0 and 100°C leads that these block copolymers present amphiphilic features accompanied by surface-active properties (Herzberger *et al.*, 2016). An example of a commercial product is the poloxamer 188, that is sold like poloxamer PI88 but also like Pluronic<sup>®</sup> F68 and Kolliphor<sup>®</sup> PI88, which is used in cell culture (mammalian, insect and plant) because it can control shear forces and confer cryoprotection in suspension cultures (Barbulescu, Burton e Salisbury, 2011; Chang *et al.*, 2017).

Pluronics<sup>®</sup> are known by your amphiphilic features, but also for your temperature sensitivity, being able to produce thermoreversible gels, some already approved by the FDA and EPA for applications as food additives, pharmaceutical ingredients, drug delivery carriers and also as materials for tissue engineering (Aguilar *et al.*, 2007). These polymers exhibit a sol-gel transition around 37°C (physiological temperature) and gel-sol transition around 50°C (Aguilar *et al.*, 2007; Herzberger *et al.*, 2016).

The nomenclature of Pluronic<sup>®</sup>, Synperonic<sup>®</sup> and Lutrol<sup>®</sup> includes the letters, F, P, or L, associated to the state solid, paste and liquid, respectively, followed by a two or three digits as a numeric code (Kabanov, Zhu e Alakhov, 2005; Prhashanna, Khan e Chen, 2015). The numeric codes have relation with the structural parameters, where the last digit translates the PEO content in tens of weight percent (e.g. 50% wt. if the digit is 5) (Kabanov, Zhu e Alakhov, 2005; Prhashanna, Khan e Chen, 2015). The first one or the two digits translate the molecular mass of the PPO, where it is necessary to multiply the corresponding number by 300 (e.g. The PO block of L6I has an MW of  $300 \times 6 = 1800\text{Da}$ ) (Kabanov, Zhu e Alakhov, 2005; Prhashanna, Khan e Chen, 2015). Therefore, it is necessary to understand that the term “poloxamer” corresponds to the nonproprietary name, and Pluronic<sup>®</sup> and poloxamers have different nomenclatures (Herzberger *et al.*, 2016; Singh-Joy e McLain, 2008; Torcello-Gómez *et al.*, 2014). In this sense, poloxamers start with letter 'P' followed by one or two digits associated with the approximate molecular weight of the PPO block when multiplied by a factor of 100 (Herzberger *et al.*, 2016; Torcello-Gómez *et al.*, 2014). While the last digit has the same meaning than the one presented for Pluronic<sup>®</sup> (Herzberger *et al.*, 2016; Torcello-Gómez *et al.*, 2014). (see Table 3)

Table 3 - Physicochemical characteristics of Pluronic® and poloxamer block copolymers. Adapted (Herzberger et al., 2016; Kabanov, Batrakova e Alakhov, 2002; Singh-Joy e McLain, 2008; Torcello-Gómez et al., 2014)

Pluronic	Poloxamer	MW <sup>a</sup>	Average number of EO units(x) <sup>b</sup>	Average number of PO units(x) <sup>b</sup>	HLB <sup>c</sup>	Cloud point in 1% aqueous solution (°C) <sup>c</sup>	CMC (M) <sup>d</sup>
L35	P105	1900	21.59	16.38	19	73	5.3 × 10 <sup>-3</sup>
L43	P123	1850	12.61	22.33	12	42	2.2 × 10 <sup>-3</sup>
L44	P124	2200	20.00	22.76	16	65	3.6 × 10 <sup>-3</sup>
L61	P181	2000	4.55	31.03	3	24	1.1 × 10 <sup>-4</sup>
L62	P182	2500	11.36	34.48	7	32	4.0 × 10 <sup>-4</sup>
L64	P184	2900	26.36	30.00	15	58	4.8 × 10 <sup>-4</sup>
F68	P188	8400	152.73	28.97	29	>100	4.8 × 10 <sup>-4</sup>
L81	P231	2750	6.25	42.67	2	20	2.3 × 10 <sup>-5</sup>
P84	P234	4200	38.18	43.45	14	74	7.1 × 10 <sup>-5</sup>
P85	P235	4600	52.27	39.66	16	85	6.5 × 10 <sup>-5</sup>
L92	P282	3650	16.59	50.34	6	26	8.8 × 10 <sup>-5</sup>
F98	P288	13000	236.36	44.83	28	>100	7.7 × 10 <sup>-5</sup>
L101	P331	3800	8.64	58.97	1	15	2.1 × 10 <sup>-6</sup>
P103	P333	4950	33.75	59.74	9	86	6.1 × 10 <sup>-6</sup>
P104	P334	5900	53.64	61.03	13	81	3.4 × 10 <sup>-6</sup>
P105	P335	6500	73.86	56.03	15	91	6.2 × 10 <sup>-6</sup>
P108	P338	14600	265.45	50.34	27	>100	2.2 × 10 <sup>-5</sup>
L121	P401	4400	10.00	68.28	1	14	1.0 × 10 <sup>-6</sup>
P123	P403	5750	39.20	69.40	8	90	4.4 × 10 <sup>-6</sup>
F127	P407	12600	200.45	65.17	22	>100	2.8 × 10 <sup>-6</sup>

<sup>a</sup> The Average molecular weights provided by the manufacturer (BASF, Wyandotte, MI).

<sup>b</sup> The average numbers of EO and PO units were calculated using the average molecular weights.

<sup>c</sup> HLB values of the copolymers; the cloud points were determined by the manufacturer.

<sup>d</sup> CMC values were determined previously using pyrene probe. (Kabanov, Batrakova e Alakhov, 2002)

### 1.2.1.2.1 Pluronic (Poloxamer) L64

L64 is a type of poloxamer with a molecular weight of 2900Da and an HLB of 15, being water soluble (Kabanov, Batrakova e Alakhov, 2002) (see Table 3). The L64 is constituted by 30 PPO units in the middle, and 13 PEO units on each side (Mata et al., 2005) (see Figure 3). As happens with the other poloxamers, Pluronic L64 has the capacity to form micellar systems at

determined concentration and temperature (Mata *et al.*, 2005; Prhashanna, Khan e Chen, 2015; Roques *et al.*, 2009). In order to obtain the aggregation of unimers of Pluronic L64 in micelles, it is necessary to have a concentration above the critical micelle concentration (CMC), that is  $4.8 \times 10^{-4}$  mol/L in an aqueous solution at 37°C (Kabanov, Batrakova e Alakhov, 2002; Kozlov *et al.*, 2000). Although, to prepare micellar systems with Pluronic L64, not only the concentration of polymer has influence, but also the temperature and the type of solution used (aqueous, saline) (Mata *et al.*, 2005; Prhashanna, Khan e Chen, 2015; Roques *et al.*, 2009). The critical micelle temperature (CMT) is another parameter extremely important in the development of micelles, because, in the case of L64, an increase in the temperature reduces the CMC (Roques *et al.*, 2009). Another point that should be considered is the fact that the use of saline solutions alters the CMC and CMT, decreasing them (Mata *et al.*, 2005; Roques *et al.*, 2009).

During the past years, this polymer has been used in several research works, presenting good results in areas like drug and gene delivery. Moreover, it has been used, associated with cholesterol, for production of niosomes with thermo-sensitive properties for drug delivery (Tavano *et al.*, 2016). Relatively to gene delivery, it is proved that an optimal concentration of L64 achieve the endosomal/lysosomal escape because it enhanced the permeability of biomembranes through structural disturbance and pore formation (Chen *et al.*, 2015). Another work demonstrated that formulations with Pluronic L64 induce efficient gene transfer to dystrophic muscles of CHF147 Syrian hamsters (Roques *et al.*, 2009).

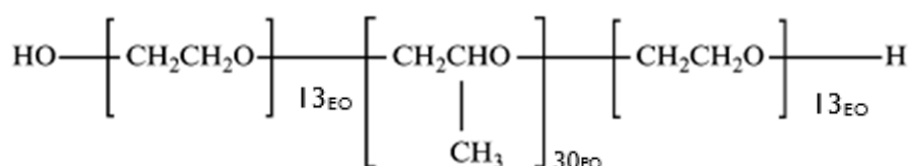


Figure 3 - Pluronic L64 block copolymer contain two hydrophilic EO blocks and a hydrophobic PO block. Adapted (Kabanov, Zhu e Alakhov, 2005).

### 1.2.1.3 Polymeric micelles

Polymeric micelles were considered one of the most promising drug carrier systems in the 1990s, however, the number of published works using polymeric micelles as nanosystems to deliver drugs and nucleic acids just presented a faster increase since 2000 (Yokoyama, 2014).

Polymeric micelles are macromolecular assemblies formed by the self-aggregation of amphiphilic copolymers, mostly having two or three synthetic blocks of copolymers, like poloxamers and poloxamines, or graft copolymers with different hydrophobicity (Simões *et*

*al.*, 2015). The formed micelles possess a two-phase structure with a spherical inner core constituted by hydrophobic blocks and an outer shell constituted by hydrophilic units, as shown in Fig. 2 (Cagel *et al.*, 2017; Simões *et al.*, 2015; Xiong *et al.*, 2011; Yokoyama, 2014).

They are nano-sized structures, normally between 10 and 200 nm, that have the capacity to self-assemble in a micellar structure above the CMC (Cagel *et al.*, 2017; Simões *et al.*, 2015; Yokoyama, 2014). In other words, when the concentration of the polymer remains above the CMC, the formed micelles are thermodynamically stable, but once the concentration decreases below the CMC, micelles disintegrate depending on the amphiphilic structure and the interaction between the chains (Yokoyama, 2014). CMC values can be calculated by different methods like conductivity, fluorescence spectroscopy (e.g. pyrene probe), surface tension (e.g. Wilhelmy plate method), scattering techniques (e.g. DLS), calorimetry, voltammetry, and UV/vis spectroscopy (Esteves *et al.*, 2016; Mohr *et al.*, 2007; Topel *et al.*, 2013). The method of pyrene is widely used and it is based on the quantification of the fluorescence emitted by the pyrene probe, which is based on the change of the intensity ratio of peaks I/III (peak I with  $\lambda_{\max} = 373\text{nm}$  and peak III with  $\lambda_{\max} = 383\text{nm}$ ) as a function of the surfactant concentration (Mohr *et al.*, 2007).

As aforementioned for Pluronic L64, beyond CMC, poloxamers have another critic factor that can affect their micellization, namely the CMT (Batrakova e Kabanov, 2008; Jung *et al.*, 2013; Kabanov, Batrakova e Alakhov, 2002; Kabanov, Zhu e Alakhov, 2005). In the case of poloxamer micelles, the association and dissociation of the hydrophilic and hydrophobic blocks, at a certain concentration, is temperature-sensitive (Jung *et al.*, 2013). Poloxamers only form micelles, when they become more lipophilic, exceeding their CMT (Jung *et al.*, 2013; Kabanov, Batrakova e Alakhov, 2002; Kabanov, Zhu e Alakhov, 2005). It is proved that a higher CMT is associated with a lower molecular weight and a higher content of PEO units, consequently, lower values of CMC and CMT are obtained with a high content of hydrophobic blocks (PPO) (Herzberger *et al.*, 2016). In another side, when comparing similar EO/PO ratios, copolymers with a high molecular weight present low values of CMC and CMT (Chiappetta e Sosnik, 2007).

Regarding this, polymeric micelles, in an aqueous medium, are characterized by a core-shell architecture, in which the hydrophobic core can act as a drug-loading site, creating a space for the encapsulation of hydrophobic drugs through the establishment of physical or chemical interactions (Alvarez-Lorenzo *et al.*, 2012; Xiong *et al.*, 2011; Yokoyama, 2014). The properties of the outer shell and inner core have an influence in the drug and nucleic acids release, which can promote an easier or hampered release (Simões *et al.*, 2015).

They have the ability to escape from a non-specific capture by the reticuloendothelial system (RES), mainly because the hydrophilic shell minimizes the interaction with serum proteins and, consequently, their cellular adhesion (Alvarez-Lorenzo *et al.*, 2012; Cagel *et al.*, 2017). Polymeric micelles also have a size that is above the threshold for filtration by kidneys (Cagel *et al.*, 2017; Xiong *et al.*, 2011; Yokoyama, 2014).

In relation to poloxamers, the efficiency of evasion depends on the composition of the PEO–PPO copolymers and on the molecular weight, taking into account that copolymers highly hydrophilic with a high molecular weight produce micelles with a shield effect more effective (Herzberger *et al.*, 2016).

According to this, polymeric micelles have potential to transport several drugs and nucleic acids, improving the circulation time, as well as, demonstrating an enhanced permeability and retention (EPR) effect, which, subsequently, promotes the passively accumulation in sites with high vasculature, such as solid tumors and sites of inflammation (Alvarez-Lorenzo *et al.*, 2012; Cagel *et al.*, 2017; Simões *et al.*, 2015; Xiong *et al.*, 2011; Yokoyama, 2014). Moreover, these systems are considered to exhibit low-risk of chronic toxicity since polymeric micelles are disassembled *in vivo*, in a single polymer chain that can be excreted by kidneys (see Figure 4) (Yokoyama, 2014).

Different types of polymeric micelles can be developed, depending on the structure of the amphiphilic copolymer used and the solution parameters (polymer concentration, solvent type, pH, ionic strength, temperature, solvent/cosolvent ratio and others) (Simões *et al.*, 2015). In this way, it can be obtained diverse micelle-like structures with different morphology, which is important to a range of advanced applications in nanotechnology (Rizis, Ven, Van De e Eisenberg, 2014).

Relatively to poloxamers, the length of the PEO and PPO block will affect the micelle shape (Torcello-Gómez *et al.*, 2014). By rule, the simplest approach is the achievement of spherical micelles when it is used a polymer with a hydrophilic block longer than the hydrophobic (Simões *et al.*, 2015; Venkataraman *et al.*, 2011). Lamellar structures are, normally formed at high concentrations and high temperatures presenting longer hydrophobic blocks (Torcello-Gómez *et al.*, 2014). Besides this, with longer hydrophobic blocks can be obtained rod or polymeric vesicles (polymersomes) (Nascimento, do *et al.*, 2016; Rizis, Ven, Van De e Eisenberg, 2014). The use of triblock copolymers allows the production of “flower-like” polymeric micelles, constituted by small hydrophobic ends and a long hydrophilic chain, but also gives the chance to have micelles with several well-differentiated compartments (Graaf, de *et al.*, 2011; Trivedi e Kompella, 2010).

In another context, it is possible to revert the hydrophilic properties of the shell to the core, being produced reverse polymeric micelles, for this it is necessary to use a non-aqueous medium in order to obtain a shell more hydrophobic and a core more hydrophilic (Simões *et al.*, 2015; Trivedi e Kompella, 2010). The use of copolymers with cationic chains and copolymers with hydrophobic chains makes possible the formation of polymeric micelles with cationic properties that can interact with DNA/RNA molecules to form micelleplexes (see Figure 4) (Wang *et al.*, 2016). The micelleplexes are included in the polyion complex micelles, but they can contain other substances besides nucleic acids, such as metal ions and enzymes (Ohno, Ishihara e Yusa, 2016). In the case of poloxamers, it is necessary a conjugation with a cationic polymer in order to form a polyion complex micelle (Li *et al.*, 2014).

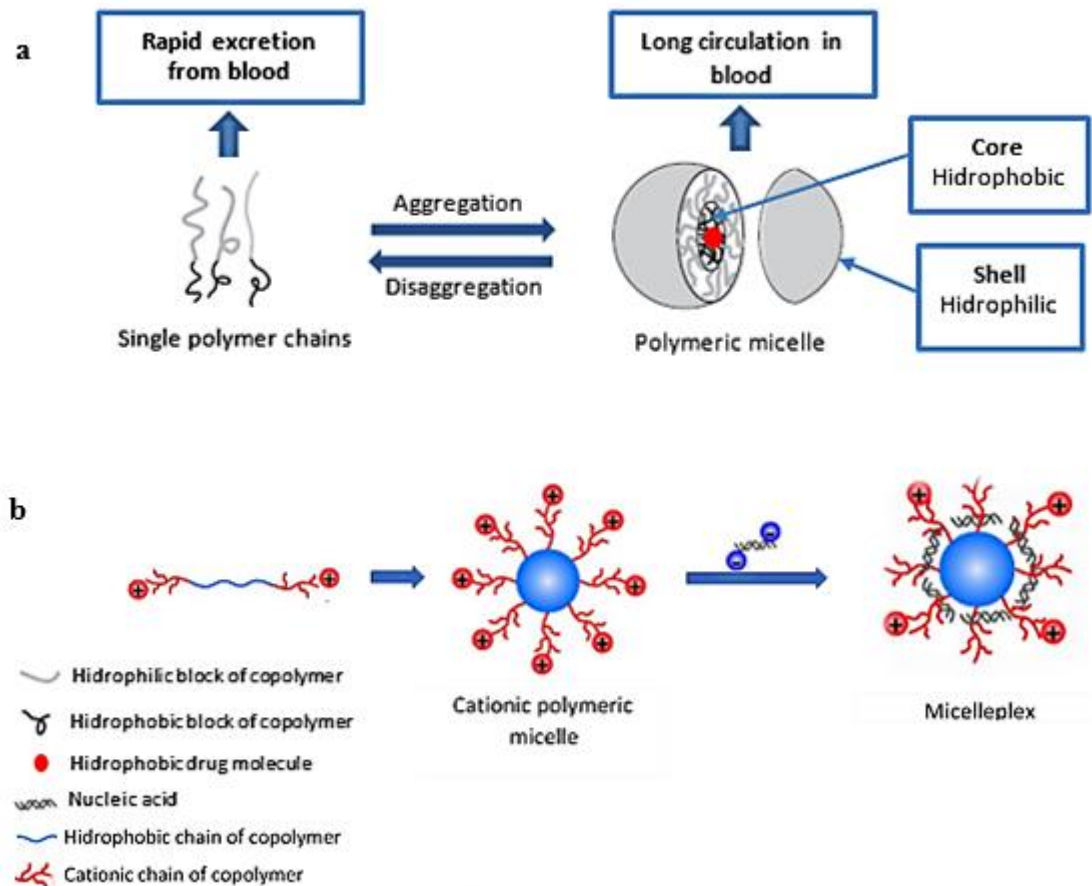


Figure 4 - Polymeric micelles as (a) drug and (b) nucleic acid (micelleplex) delivery systems. Adapted (Wang *et al.*, 2016).

### 1.2.1.3.1 Micelleplexes

A recent concept designed by micelleplex was introduced in nanomedicine. This term is respective to a linkage between an amphiphilic copolymer and a cationic polymer, in which they can self-assemble to form polymeric micelles with cationic properties (Chitkara, Singh e Mittal, 2016). These micelleplexes have the same characteristics of a polymeric micelle, with an additional feature that are associated with the cationic properties, making possible the interaction with nucleic acids (Pereira *et al.*, 2017).

The micelleplexes are multifunctional micelles due to the possibility to encapsulate poorly water-soluble drugs, in the inner core, and nucleic acids, in the positively charged corona, at the same time (Jhaveri e Torchilin, 2014; Pereira *et al.*, 2017). In fact, these structures bring additional advantages, like the contribution of both hydrophobic and electrostatic interactions to micelleplex formation and stability, but also the possibility to obtain a combined therapy (drug and nucleic acid delivery), using the same system (Zhang *et al.*, 2016).

In this way, it is necessary to have in consideration the difference between polyplexes and micelleplexes, which are not differentiated by many authors. This is, both polyplexes and micelleplexes are associated with the capacity to perform electrostatic interactions with nucleic acids, however, micelleplexes are produced by compounds with cationic and amphiphilic properties that can aggregate to form micelles, whereas the polyplexes do not form micelles (Gary *et al.*, 2011).

The term micelleplex concerns the formation of a micellar structure that interacts with nucleic acids, being also able to encapsulate other compounds like drugs. Therefore, to have an efficient interaction between the genetic material and the cationic polymer, it is necessary taking into account the optimal ratio between the nitrogen (N) content in the cationic polymer and the phosphate (P) content in the nucleic acid, commonly designated as N/P ratio (Wang *et al.*, 2016).

Different micelleplexes have been developed over the years, not only using poloxamers but also using another type of polymers. In fact, poloxamers have the advantage to possess amphiphilic properties in order to produce polymeric micelles, despite the fact that they do not have cationic features, being necessary the conjugation with a cationic polymer.

### **1.2.1.3.1.1 Micelleplex preparation**

Precisely, the preparation of micelleplexes, by rule, involves two main steps, the first one is the micelle production, that is associated with the preparation of micelles (e.g. direct dissolution, film method, microphase separation, oil-in-water emulsion, etc.), and the second one consists in the condensation of the nucleic acids, which is related to the establishment of electrostatic interactions between the nucleic acids and the micellar complexes (Gary *et al.*, 2011). This process is necessary because free miRNA can be cleaved by serum endonucleases, causing activation of innate immunity and be recognized by the RES (Wang *et al.*, 2016; Yin *et al.*, 2014).

### **1.2.3.1.1.2 Challenges to micelleplex delivery**

Micelleplexes like other type of vectors need to possess adequate properties to transport, safely, the nucleic acids, in this particular case the miRNA, to the target cell, penetrating it and releasing the miRNA in the cytoplasm. Polymers need to have cationic features and should be biodegradable with low cytotoxicity (Mien-Chie Hung, Leaf Huang, 2014).

Thereby, the complex should be capable of transport the miRNA into the target cells, which usually can be improved through the use of ligands, such as transferrin and folate (Kim *et al.*, 2015). After reaching the cell, micelleplexes should penetrate the cell membrane by an endocytic pathway, which can be caveolae and clathrin-independent, caveolae-mediated, and macropinocytosis, depending on their size (Keles *et al.*, 2016).

After the uptake by the cell membrane, it is necessary the disruption of the endosome containing micelleplexes, because a long time in the endosome leaves to a reduction in pH, formation of the lysosome, and consequent degradation of miRNA (Yin *et al.*, 2014). Fusiogenic peptides with endosomal membrane disruptive activity and the use of polycations, such as PEI, with low pKa's, that are responsible for proton sponge effect, are some approaches to endosomal escape (Oba, 2013).

It is also required the disaggregation of miRNA from micelleplexes, and the polymers should be sensitive to degradation by the cytoplasmic enzymes (Keles *et al.*, 2016). Exists an optimal chain length and molecular weight for each polymer, used in transfection, that translate the best efficiency of nucleic acid release (Aied *et al.*, 2013).

At last, the miRNA needs to interact with RISC in order to occur mRNA cleavage or translational repression (Mokhtarzadeh *et al.*, 2017). When miRNA is free in cytoplasm it can act in different mRNA targets and/or be degraded by enzymes (Tomaselli *et al.*, 2013). (Figure 5)

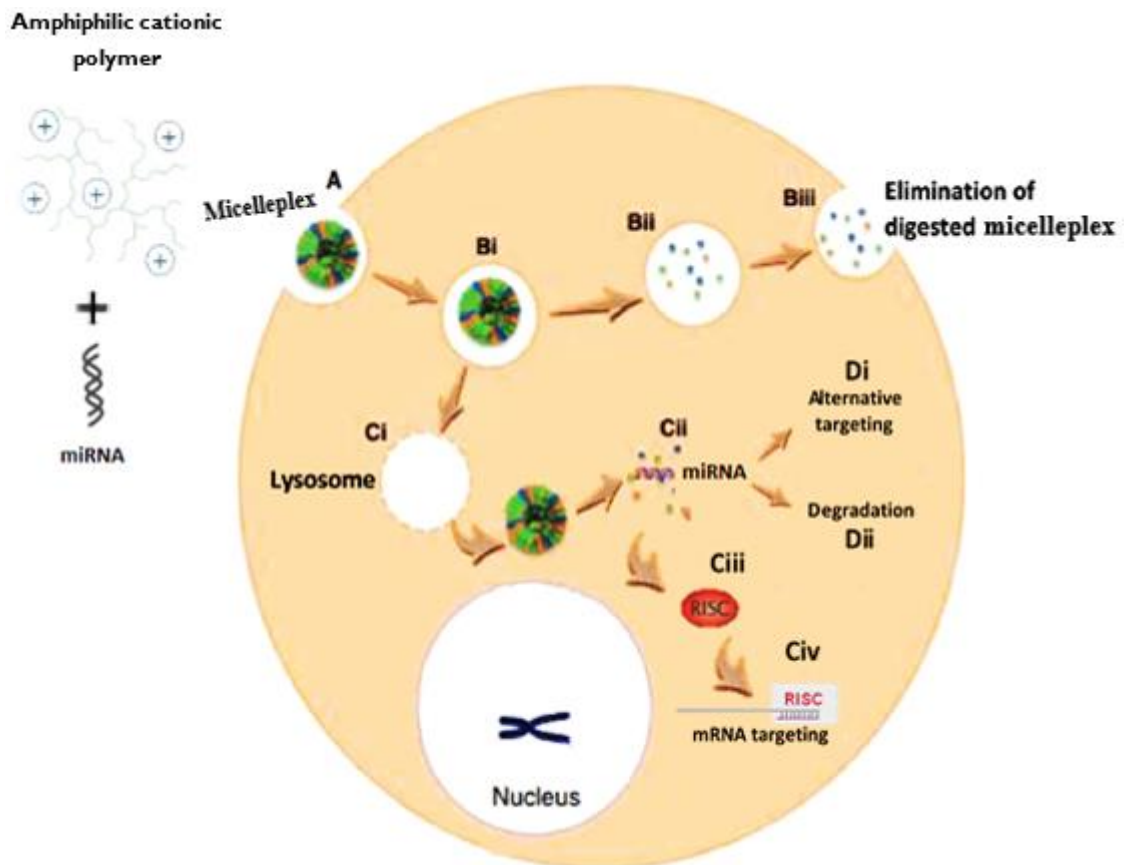


Figure 5 - Stages of intracellular miRNA delivery. (A) Micelleplex interaction with the cell membrane results in the internalisation of the micelleplex by macropinocytosis, phagocytosis, or receptor-mediated endocytosis (caveolae and clathrin). (B) Formation of the early endosome (i). Micelleplexes trapped in the endosome are digested in the late endosome and/or lysosome (ii) and removed from the cell by exocytosis (iii). (C) Alternatively, if the micelleplex induces endosomal escape (i), it travels through the cytoplasm, where the polymer is gradually degraded by cytoplasmic or intracellular enzymes (ii). miRNA binds to RNA-induced silencing complex (RISC) (iii) and binds to mRNA target causing your cleavage or translational repression (iv). (D) Also, exists the possibility of the miRNA interacts with different mRNA targets, by alternative targeting (i) or be degraded (ii). Adapted (Aied *et al.*, 2013; Tomaselli *et al.*, 2013; Yin *et al.*, 2014)

### **1.3 Aims**

The OS is the principal type of bone cancer with a higher annual incidence rate, presenting a poor prognosis. In this sense, the available treatments to this pathology are limited, which requires a need to search for new therapeutic alternatives to overcome these limitations.

In this regard, gene therapy arises as a possible solution to respond to these constraints, being possible to produce a therapy, when a nanoparticle encapsulates genetic material with antitumoral activity. However, secure the transport through the cell barriers, and the release of sufficient amount of genetic material in target cells remains a trouble.

In this way, this work intends to develop an anticancer gene therapy strategy to act in OS. This involves two main objectives. The first one is the development and full characterization of a poly(ester amine) (PEA), composed of Pluronic L64-PEI, that can self-assemble to form a micellar structure. The second aim is the encapsulation of the miR-145 in the prepared system in order to form a micelleplex that can penetrate the membrane, of OS cells, to release an efficient quantity of miR-145, in the cytoplasm, to obtain a therapeutic action.

## 2 Material and Methods

### 2.1 Materials

Pluronic L64 (Mw=2900Da), benzene anhydrous, hexane, anhydrous dichloromethane, deuterium oxide (D<sub>2</sub>O), resazurin sodium salt, and rhodamine B isothiocyanate mixed isomers were purchased from Sigma-Aldrich (St. Louis, MO, USA). PEI branched 99% (Mw=1800Da) and acryloyl chloride were purchased from Alfa Aesar. Triethylamine was purchased from Merck. Water for molecular biology, Agarose Electrophoresis grade, and Green Safe were provided by Nzytech (Lisbon, Portugal). DMEM-HG medium was acquired by Biowest (Nuaille, France), Fetal Bovine Serum (FBS), Penicillin-Streptomycin (Pen-Strep) and Trypsin-EDTA were purchased from Sigma-Aldrich (St. Louis, MO, USA). The miR-145 mimic and miR non-target were purchased from Active Motif (Carlsbad, CA, USA) and the Annexin V Apoptosis Detection Kit with PI was purchased from BioLegend (San Diego, CA, USA). MG-63 cell line was a kind gift from Prof. Maria Helena Fernandes (Faculty of Dentistry, University of Porto) and COS-7 cell line was kindly provided by Dr. Célia Cabral (CNC/IBILI, Faculty of Medicine, University of Coimbra).

### 2.2 Synthesis of Pluronic L64 Diacrylate

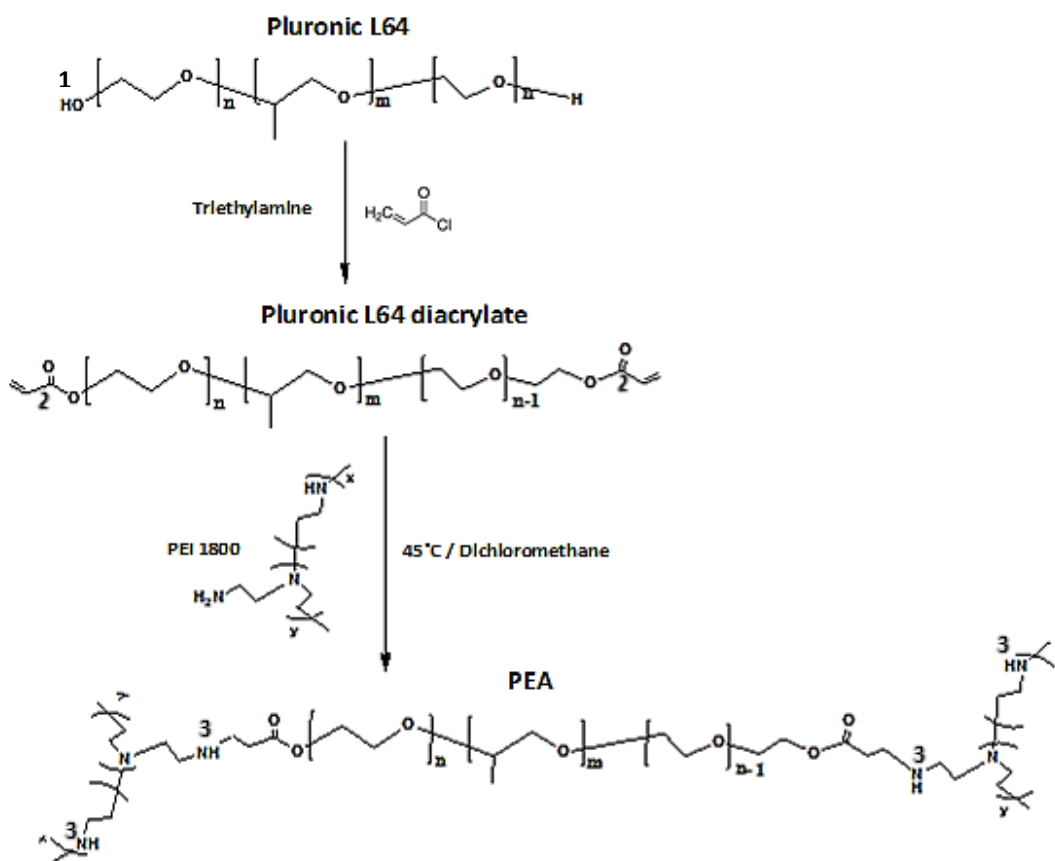
Pluronic L64 (MW=2900Da) was end-capped with acrylate groups, as previously described (Kim *et al.*, 2007). It was weighted 15.125 g of Pluronic L64 in an Erlenmeyer and after it was added 60 ml of benzene anhydrous to dissolve completely the Pluronic L64. The solution was transferred to a triple neck round bottom flask. This flask was placed in a heated plate coupled to a condenser and secure in a lab stand with claws. Then, 2.75 mL of triethylamine and 1.60 mL of acryloyl chloride were added to the flask. A magnet was added to the flask and the mixture was stirred, magnetically, for 3 h at 80°C. In one of the necks of the round bottom flask was placed a thermometer for temperature control. In the end of the reaction, the product was filtrated in a filtration plate to remove triethylamine-hydrochloride. The round bottom flask was placed in the rotary evaporator in order to evaporate the benzene. To precipitate the product, it was necessary dropping the product into 250mL of cold hexane (previously cooled in ice), under stirring, to a round-bottom flask. At last, to separate the diacrylate poloxamer from the hexane, the solution was filtrated in a filtration

plate, and the precipitated was dried in a vacuum shelf dryer at 40°C under reduced pressure, until use. (scheme 1)

### **2.3 Synthesis of cationic PEA complexes (L64 diacrylate + PEI)**

The PEAs were synthesized by Michael addition, in which the branched PEI was conjugated to Pluronic L64 diacrylate. Three different molar ratios of L64 diacrylate to PEI (1/10, 2/10, 3/10) were tested. The PEAs were designed like PEA 1 (1/10), PEA 2 (2/10) and PEA 3 (3/10). It was weighted 0.322g, 0.644g and 0.967g of poloxamer diacrylate in different Erlenmeyers for each ratio (1/10, 2/10, 3/10), respectively. The same amount of 2 g of PEI was weighted in different round bottom flasks. All the products were dissolved, separately, with 6 mL of anhydrous dichloromethane. After that, the poloxamer diacrylate was added to each PEI solution under stirring. The round bottom flasks containing each solution were placed in a Radleys carrousel, for parallel synthesis, and coupled to condensers and secured in a lab stand with claws (figure 6). The temperature was set to 45°C, during 48h. Then each round bottom flask was put in a rotary evaporator at 40°C under reduced pressure, for 15 minutes, for anhydrous dichloromethane evaporation. In order to dry and for the total elimination of the anhydrous dichloromethane the flasks were placed under high vacuum overnight. The products were put in vials, sealed and stored in the fridge in a desiccator.

A part of each total product, 0.5 g, was weighted in different beakers (one for each ratio) and dissolved, under magnetic stirring, in 10 mL of distilled water. The solution was subjected to dialysis with a membrane (MWCO=6000-8000 Da) against distilled water, for 24h in the fridge under magnetic stirring, to remove the unreacted PEI and other small molecules. The dialyzed, inside the membrane, was divided in Falcons of 15mL and frozen. At last the frozen solutions were lyophilized and stored, at the fridge, in a desiccator. (scheme 1)



Scheme 1 - Synthesis of Pluronic L64-PEI (PEA) copolymers. The numbers 1, 2 and 3 represent functional groups.

## 2.4 Preparation of PEA micelles

The PEA micelles were prepared by direct dissolution in distilled water. The stock solutions of PEA were prepared with a final concentration of 1 mg/mL, whereas the specific amount of PEAs was measured and dissolved in distilled water, under magnetic stirring, for 1 hour. The necessary dilutions were performed, and the solutions were filtrated with a filter of 0.2  $\mu\text{m}$ . The final solution of PEA was incubated for 30 minutes and then used.

## 2.5 Micelleplexes preparation

This procedure was realized in sterile conditions. All the solutions used in this part were prepared with RNase-Free water. The micelleplexes were prepared by complexation between negative phosphate groups (P) of RNA and positive amino groups (N) of PEA polymer and their preparation had into account the different N/P ratios used, namely 1/1, 5/1, 10/1.

Thus, in a first phase, it was realized an optimization of the different PEAs formulations, in order to choose the best molar ratio of PEA, which was performed by using a small RNA with 180 base pairs.

Briefly, micelleplexes were developed in HEPES-buffered saline (HBS) (100 mM of NaCl, 20 mM of HEPES, pH 7.4), where it was added the correspondent volume of each amount of the miRNA solution to each PEA solution, taking into account the N/P ratio used. After the addition of miRNA, the solutions were vortexed for 30 seconds and incubated for 30 minutes at room temperature. Micelleplexes were used right away.

## **2.6 Conjugation of micelleplexes with Rhodamine-B**

This procedure was realized with the fluorescent probe Rhodamine B isothiocyanate (RITC). For this purpose, RITC was bounded to PEA based on the protocol of Sunoqrot and colleagues (Sunoqrot *et al.*, 2011).

Firstly, it was dissolved 5.4 mg of rhodamine ( $1.0 \times 10^{-5}$  mol) in 1 mL of pure water and added to PEA ( $2.0 \times 10^{-6}$  mol) dissolved in 4mL of pure water. The pH of the mixture was adjusted to 9.0 using 1M of sodium hydroxide (NaOH) solution, followed by vigorous mixing at room temperature for 24 h. The unreacted rhodamine was removed using a membrane dialysis (OrDial D80 dialysis membrane, MWCO 6000-8000, Orange Scientific) against phosphate buffered saline (PBS) for 2 days, changing the buffer every 12 h, followed by dialysis in pure water for 2 days, changing the water every 12 h. The purified conjugates were lyophilized using Telstar LyoQuest and stored at  $-20$  °C.

## **2.7 Complexes characterization**

### **2.7.1 Particle size, zeta potential, and molecular weight**

The mean particle diameter of the PEAs and micelleplexes, polydispersion index, zeta potential and molecular weight were determined using a Zetasizer Nano-ZS (Malvern Instruments Inc., Worcestershire, UK). The mean particle diameter and polydispersion index were determined by dynamic light scattering (DLS), with a He-Ne laser (4 mW, 633 nm) light source and a  $173^\circ$  angle scattered light collection configuration. Each sample was equilibrated for 1 minute at  $25^\circ\text{C}$ . The zeta potential of the complexes was determined by laser Doppler electrophoresis, at  $25^\circ\text{C}$ . The average values of particle diameter and surface charge (zeta

potential) were calculated with the data obtained from three measurements  $\pm$  SD. The molecular weight was also determined, by static light scattering, at 25°C.

### **2.7.2 <sup>1</sup>H-NMR spectroscopy**

Solutions of all polymers PEAs, PEI, Pluronic L64 and Pluronic L64 diacrylate were prepared in 250 $\mu$ L of D<sub>2</sub>O and their composition was estimated by proton nuclear magnetic resonance (<sup>1</sup>H-NMR) spectroscopy, using the Bruker Avance III of 400 MHz. The spectra were treated with NUTS NMR Data Processing Software.

### **2.7.3 Fourier transform-infrared spectroscopy (FTIR)**

Spectra were recorded using a Jasco FT/IR-420 spectrometer associated with an ATR horizontal reflexion (Miracle<sup>TM</sup>, PIKE Technologies). Spectra acquisitions were performed in lyophilized samples with the application of 16 scans at a resolution of 4 cm<sup>-1</sup> over the range 4000-650 cm<sup>-1</sup>.

### **2.7.4 Transmission Electron Microscopy**

The morphology of PEAs micelles and micelleplexes were evaluated by transmission electron microscopy (TEM). For the morphology characterization, 5  $\mu$ l of PEA solution was placed on a copper grid covered with a polymer film (Formvar), while for micelleplexes, before this step, the copper grids suffer a chemical treatment with Alcian Blue. The samples were observed in the electron microscope, Tecnai G2 Spirit BioTWIN (FEI Company, Eindhoven).

## **2.8 Agarose gel electrophoresis assay**

The binding affinity of RNA to PEA micelle complexes was evaluated by an agarose gel electrophoresis assay.

The micelleplexes were prepared as previously mentioned. Gels were prepared with 1% of agarose and run at 100mV for 45 minutes in 1X TBE buffer (89 mM Tris, 89 mM boric acid, 2 mM EDTA). The gels were stained with Green safe and loading buffer was added to each sample. The gel images were obtained on a Bio-Rad Gel Doc XR (Bio-Rad Laboratories, Hercules CA) with Quantity One imaging software.

### 2.8.1 Quantification method

The quantification of binding affinity of the samples was analysed by Gel Quant Express software using the gel captured images (Clima *et al.*, 2015). Typically, in the gel was run a reference, RNA, whose intensity was quantified by the software as 100%. To determine the maximum loading capacity of RNA on PEA micelles, the signal intensity value of unbound RNA was determined by comparing the band intensity of the reference signal and the band intensity of the unbound RNA of the sample. The encapsulation efficiency E (%) was determined by:

$$E = 100 - I_{sb}$$

where 100% refers the intensity of reference signal (RNA), and the  $I_{sb}$  (%) refers the intensity of the sample bands in the gel image that represents the unbound miRNA.

## 2.9 Cell culture

It was used two cell lines, COS-7 cell line that corresponds to fibroblast-like cell lines derived from green monkey kidney tissue and MG-63 cell line, a human osteosarcoma cell line. Both the cell lines were maintained in culture with DMEM-HG (Dulbecco's modified Eagle's medium - high glucose) that was supplemented with 10% fetal bovine serum (FBS) and 1% of penicillin-streptomycin. Cells were maintained at 37°C and 5% of CO<sub>2</sub>.

### 2.9.1 Binding and uptake assay

The binding and uptake of micelleplexes by cell membrane were determined by a fluorometric method, using the fluorescent probe Rhodamine B isothiocyanate. The intensity of fluorescence determines the extent of binding and uptake of micelleplexes by the cells. The labeling of micelleplexes with Rhodamine B isothiocyanate is described in topic 2.6. The micelleplexes with Rhodamine B isothiocyanate were prepared as it was referred previously, at two N/P ratios, 5/1 and 10/1. The final concentration used for miR-145 mimic was 10 and 50 nM and micelleplexes were prepared to a final volume of 300 µL.

For this assay, it was used the MG-63 cell line. This cell line was seeded, in 48 well plates,  $4 \times 10^4$  cells per well 24 hours before the assay. After that, it was retired the medium and it was added 200 µL of medium to each well. Then, the plates were incubated at 37°C for 30 minutes. After that, one plate was incubated at 4°C and the other plate was incubated at 37°C for 30 minutes. Subsequently, it was added the RITC-micelleplexes solutions to the two plates and they were incubated during 3 hours at 4°C and 37°C to evaluate the binding and

uptake, respectively. At last, the cells were washed twice with PBS (phosphate buffered-saline) and lysed with 1% Triton X-100 solution. The fluorescence was measured with a fluorometer (Synergy™ HT Multi-Mode Microplate Reader, BioTek Instruments), using the excitation wavelength of 530nm and the emission wavelength of 590nm.

### **2.9.2 Cell death assessment**

The cell death assessment was realized after the transfection with micelleplexes, in MG-63 cell line. Two assays were performed: cell viability 24 and 48 hours after transfection and flow cytometry 48 hours after transfection. The micelleplexes were prepared at two N/P ratios 5/1 and 10/1. The final concentration used for miR-145 mimic was 10 and 50nM. Besides this, it was also prepared a negative control: micelleplexes with a concentration of 50nM of miR “non-target”.

The goal of this assay was to evaluate the antitumor activity of micelleplexes. For flow cytometry assay, the micelleplexes were prepared to a final volume of 500µL and for viability assay were prepared to a final volume of 300µL.

The cells were plated with 80% of confluence, in order to secure that cells were in your exponential growth phase. For flow cytometry, the cells were plated in a 12 well plate at a density of  $8 \times 10^4$  cells per well and for cell viability, cells were plated in a 48 well plate at a density of  $4 \times 10^4$  cells per well. The micelleplexes were added to the cells and incubated for 4 hours, and after that, it was aspirated the medium of the plates and it was added new medium to each well.

#### **2.9.2.1 Flow cytometry**

Flow cytometry was used to evaluate the cell death through the Annexin V/PI assay. In this protocol, cells were simultaneously stained with Annexin V (AV), labeled with the fluorescent probe APC, and the Propidium iodide (PI). This procedure was performed according to previously reported (Mendes *et al.*, 2016).

When the cell starts to enter in apoptosis, the phosphatidylserine, a negative phospholipid, moves from the inner to the outer layer of the plasmatic membrane. Since the AV has the ability to bind to this phospholipid in the presence of calcium, it is possible to measure its expression adding a fluorochrome that binds AV. By another side, in necrosis, the cell membrane becomes highly permeable allowing small charged molecules, to which it was impermeable, to enter the cell. In this case, PI can enter the cell and intercalates DNA, leading

to an increase in its own fluorescence. Both fluorescences emitted by PI and AV can be measured by flow cytometry.

This assay allows differentiating the cell death according to fluorescence emitted: AV negative and PI negative – viable cells; AV positive and PI negative – early apoptotic cells; AV positive and PI positive – late apoptotic cells/secondary necrotic cells; AV negative and PI positive – necrotic cells.

After 48 hours of transfection, cells were co-stained with AV-APC and PI using the manufacturer's recommended protocol. Briefly, cells were washed with PBS, centrifuged at 500 Gs for 5 min, resuspended in 100  $\mu$ L of binding buffer and incubated with 5  $\mu$ L of AV-APC solution and 2  $\mu$ L of PI solution for 15 min at room temperature in the dark. After the incubation time, cells were diluted in 400  $\mu$ L of binding buffer. A six-parameter, four color FACSCalibur flow cytometer (Becton Dickinson, San Jose, CA) was used and at least 10.000 events were collected by acquisition using CellQuest software (Becton Dickinson, San Jose, CA). The results were analyzed with the Paint-a-Gate software and were expressed in percentage (%).

In order to verify the results of cytometry, after the incubation period of 48 h, cells untreated and treated with the different conditions were collected and seeded in glass slides. Then, cell smears were stained with May-Grünwald solution (0.3 %v/v in methanol; Sigma-Aldrich) for 3 min, diluted in a 1:1 ratio with distilled water, and then staining with Giemsa solution (0.75 % p/v in glycerol/methanol 1:1; Sigma-Aldrich) diluted 1:8 in distilled water for 15 min. After rinsing with distilled water, smears were left to dry at room temperature and the morphological analysis of cells was performed using a Nikon Eclipse 80i microscope equipped with a Nikon Digital Camera DXm 1200F.

### **2.9.3 Cell viability assay**

In order to evaluate if the polymers used can induce cytotoxicity, it was performed a cell viability assay in COS-7 cell line, whereas it was tested different concentrations of Pluronic L64, PEI, and all PEAs. A stock solution of 1 mg/mL was prepared for all polymers in distilled water. Final dilutions were done in HBS in 100 $\mu$ L to final concentrations of 5, 10, 20 and 40 $\mu$ g/mL. It was seeded  $3 \times 10^4$  cells per well in a 96 well plate with 100 $\mu$ L of medium and the polymer solutions were added for 24hours.

To complete the cell death assessment, a cell viability assay in MG-63 cell line was realized at 24 and 48 hours after transfection with micelleplexes.

The cell viability assay was executed using the Alamar Blue assay, which consists in a redox reaction of resazurin, that when reduced to resorufin produces a pink color (Rampersad, 2012). Metabolically active viable cells can reduce resazurin into its resorufin product, which is a pink and fluorescent compound. It was prepared a solution of 10% (v/v) of resazurin in DMEM-HG and added 200 $\mu$ L to each well. After that, the plate was incubated at 37°C until occurs a visible colour change based in the control cells (untreated). When verified the colour change, the incubation was interrupted. It was retired 150  $\mu$ L of supernatant from each well for a 96 well plate. The absorbance was measured at 570 nm and 600 nm using a spectrophotometer (Synergy™ HT Multi-Mode Microplate Reader, BioTek Instruments) and the results were normalized relative to the control.

## **2.10 Statistical analysis**

The data were analyzed with the software GraphPad Prism (version 6.0). The differences between the diverse experimental conditions were determined by one-way analysis of variance (one-way ANOVA), using the Tukey test for multiple comparisons, considering a confidence interval of 95%. It was used the t-test, two-tailed, considering a confidence interval of 95%, when comparing less than 3 conditions. The two-way analysis of variance (two-way ANOVA) was used for grouped analysis with Tukey test for multiple comparisons, with a confidence interval of 95%.

## 3 Results and discussion

### 3.1 Synthesis of Pluronic L64 Diacrylate

The synthesis of Pluronic L64 diacrylate was confirmed by FTIR and  $^1\text{H-NMR}$  spectroscopy. Through the comparison between the FTIR and  $^1\text{H-NMR}$  spectrum of Pluronic L64 with the spectrum of Pluronic L64 diacrylate, it was able to confirm the production of L64 diacrylate (see figures 7 and 8). In the L64 diacrylate FTIR spectrum, the disappearance of the band between  $3300\text{-}3600\text{ cm}^{-1}$ , related to  $\text{-OH}$  groups (confront with number 1 of scheme 1), and the appearance of a band between  $1700\text{-}1750\text{ cm}^{-1}$ , related to  $\text{C=O}$  of ester (confront with number 2 of scheme 1), confirms the formed product. In  $^1\text{H-NMR}$  spectra, also the vinyl peaks that appear in L64 diacrylate at  $\delta 5.97\text{-}6.45\text{ ppm}$ , are indicative of the formation of L64 end-capped with acrylate groups (Kim *et al.*, 2007).

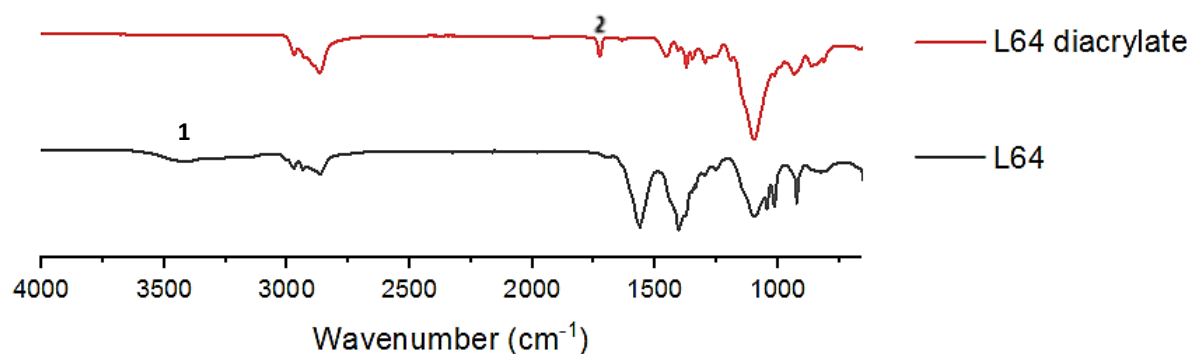


Figure 7 - FTIR spectra of Pluronic L64 and Pluronic L64 diacrylate. The numbers 1 and 2 represent functional groups (confront scheme 1).

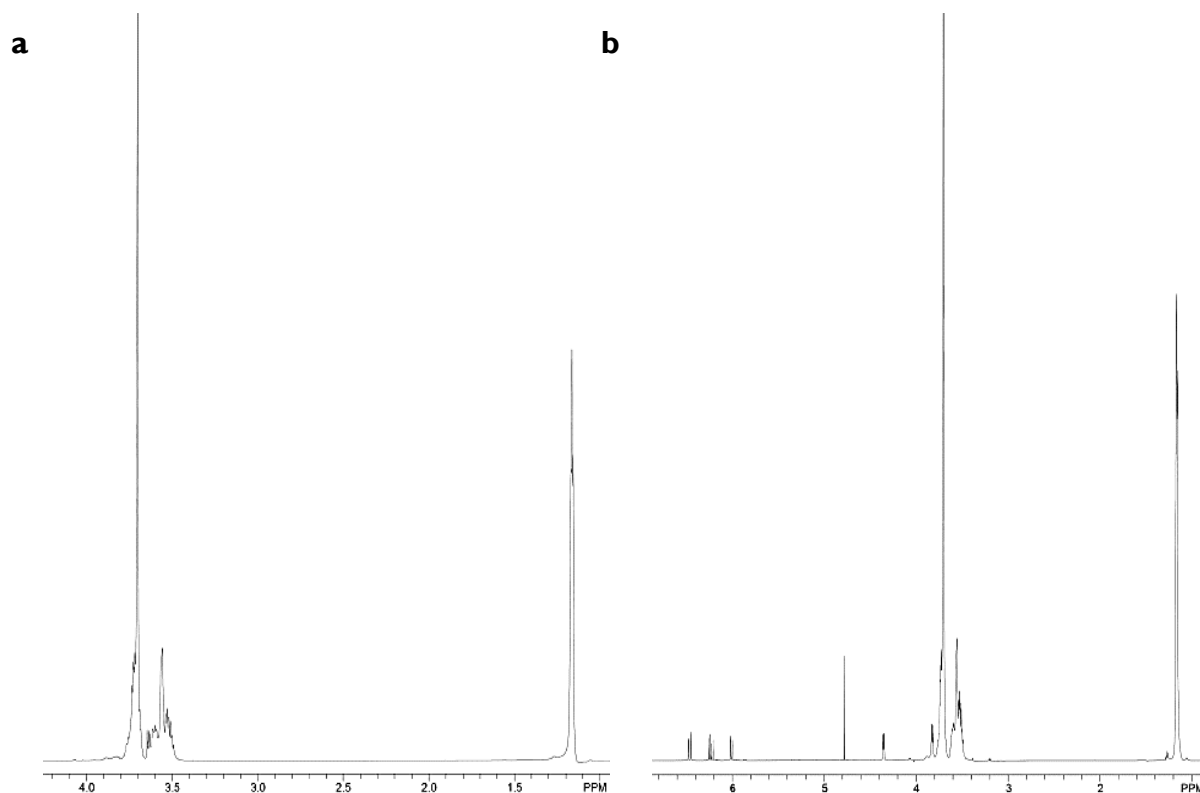


Figure 8 -  $^1\text{H-NMR}$  spectra of Pluronic L64 (a) and Pluronic L64 diacrylate (b).

### 3.2 Synthesis of cationic PEA complexes (PEI+L64 diacrylate)

The chemical structure and the functional groups of PEA complexes were analyzed by  $^1\text{H-NMR}$  and FTIR techniques. The  $^1\text{H-NMR}$  spectra of the individual polymers and the conjugated polymers, namely L64, PEI, L64 diacrylate and the final product PEA, are represented in figures 8 and 9. In  $^1\text{H-NMR}$  spectra of all PEAs, it is possible to observe the appearance of a peak between  $\delta 2.4\text{-}3.4\text{ppm}$ , that not appears in Pluronic L64 and Pluronic L64 diacrylate, which is coincident with the peak of PEI, proving the linkage between Pluronic L64 diacrylate and PEI. In FTIR spectra of all PEAs, figure 10, it is possible to verify the appearance of a band, between  $3200\text{-}3600\text{cm}^{-1}$ , coincident with the band of PEI, that corresponds to the absorption band of secondary amine groups,  $\text{-NH}$  (confront with number 3 of scheme 1).

The characteristics of all developed PEAs are described in table 4. The final molar ratio was obtained by integration of areas of  $^1\text{H-NMR}$  spectra. The peak that appears between  $\delta 2.4\text{-}3.4\text{ppm}$  in all PEAs is related to  $\text{-CH}_2\text{-CH}_2\text{NH-}$  protons of PEI and the peak at  $\delta 1.1\text{ppm}$  is related to  $\text{-CH}_3$  protons of poloxamer. The difference between the areas gives the final composition of each PEA (Kim *et al.*, 2007).

The results showed a more pronounced variation in the chemical synthesis for PEA 1, revealing that the final product does not present the final molar ratio equivalent to the amounts used. The PEA 3 also presents a soft variation, being the PEA 2 the one that presents a similar initial and final molar ratio. This can be explained by the fact that it was performed a chemical synthesis and, probably, the reaction was uncompleted. It is possible that final products presented some heterogeneity.

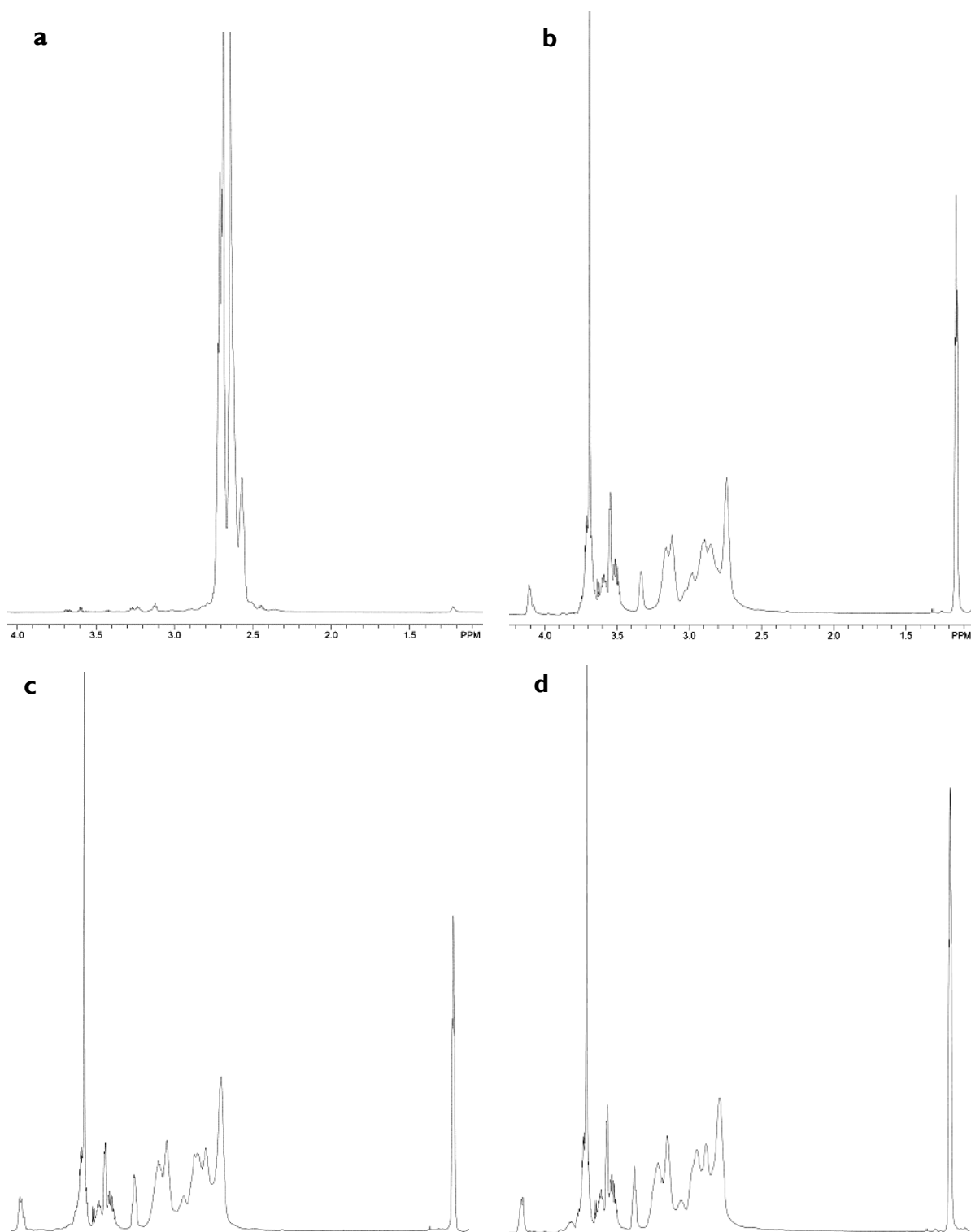


Figure 9 - <sup>1</sup>H-NMR spectra of PEI (a), PEA 1(b), PEA 2 (c) and PEA 3 (d).

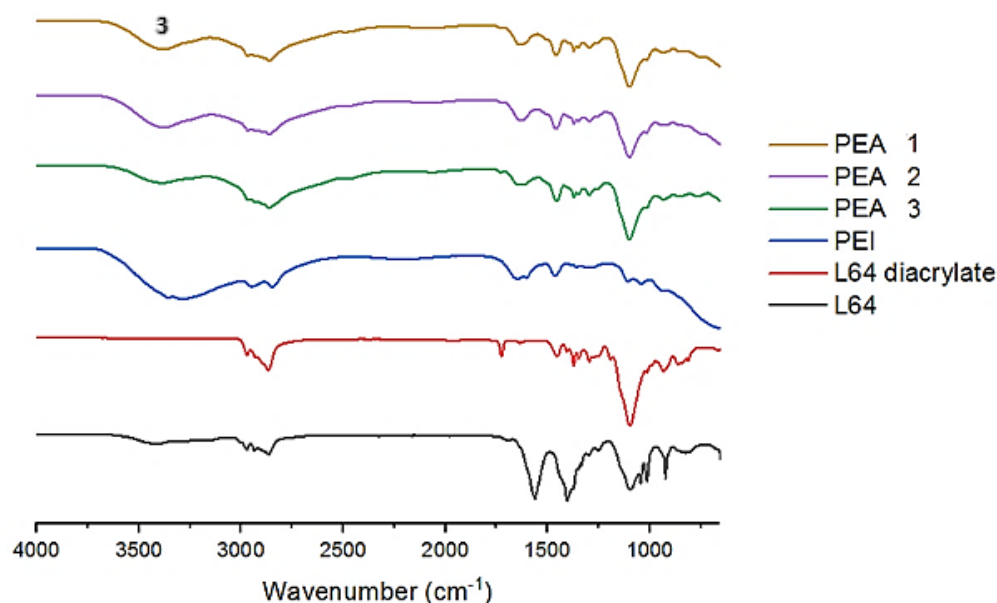


Figure 10 - FTIR spectra of Pluronic L64, L64 diacrylate, PEI, PEA 1, PEA 2 and PEA 3. The number 3 represents a functional group (confront scheme 1).

Table 4 - Characteristics of developed PEA.

Final product	MW of primary reagents		Molar ratio (Pluronic L64/PEI)	Final molar ratio (Pluronic L64/PEI) <sup>a</sup>
	Pluronic L64	PEI		
<b>PEA 1</b>	2900	1800	1/10	3.1/10
<b>PEA 2</b>	2900	1800	2/10	1.9/10
<b>PEA 3</b>	2900	1800	3/10	2.5/10

a – Determined by automatic integration of <sup>1</sup>H-NMR spectra.

### 3.3 Complexes characterization

#### 3.3.1 PEA micelles

The PEA micelles were prepared by direct dissolution and their characterization was performed in a ZetaSizer Nano ZS. The values obtained are represented in Table 5. Therefore, the results determined for size demonstrate that the bigger particles were obtained for PEA 2, although with no significant differences between the size values for all PEAs formulations.

The polydispersion index was similar to all PEAs formulations, revealing that the particle size does not vary too much between the particles formed. The results for zeta potential shows that the highest value was obtained for PEA 2 which is in accordance to the final molar ratio, because PEA 2 has the highest amount of PEI compared to the amount of poloxamer present, which means more amino groups and more positive charge. On the other side, the PEA 3 presents the smallest zeta potential, but with a huge standard deviation, revealing the heterogeneity of the final product in terms of PEI and poloxamer composition. However, all PEAs formulations revealed a high zeta potential, which is a good indicative of stability. High positive zeta potential means high positive repulsion avoiding the agglomeration (Huang *et al.*, 2017).

The results obtained for molecular weight were the expected. The molecular weight increases, PEA 1 < PEA 2 < PEA3, due to the increase in the quantity of poloxamer added to each reaction, which also happened in another two studies where it was used Pluronic L64 and PEI (Kim *et al.*, 2007; Wang *et al.*, 2016).

Table 5 - Characteristics of developed PEA, in terms of particle size, zeta potential and molecular weight.

	<b>Particle size (nm)</b>	<b>Polydispersion index (PDI)</b>	<b>Zeta potential (mV)</b>	<b>Molecular weight (Da)</b>
<b>PEA 1</b>	132.1 ± 27.49	0.316 ± 0.088	30.2 ± 4.40	14700
<b>PEA 2</b>	158.4 ± 31.74	0.309 ± 0.036	32.3 ± 5.70	30700
<b>PEA 3</b>	141.7 ± 33.45	0.281 ± 0.05	26.9 ± 14.12	53200

### 3.3.2 Micelleplexes optimization

As it was previously referred, for the optimization of the best N/P ratio to be used with miR-145, it was firstly used a small RNA of 180 base pairs, with approximately, 57849 Daltons. The micelleplexes were prepared at different N/P ratios (1/1, 5/1 and 10/1) and the results are represented in figure 11.

Confronting the results, it is possible to observe that, relatively to particle size, the N/P ratio 1/1 of PEA 1 and 2 presents the highest size and standard deviation. This can happen due to the high molecular weight of small RNA, i.e. to the possibility of one molecule of small RNA condenses two particles. An increase of the particle size means a biggest linkage of small RNA in micelle complex. As referred in a work by Akinchina and Linse, with a large polyion charge, in this case a large small RNA, only a part can involves one micelle, being possible the

other part involves other micelle, producing large micelleplexes (Akinchina e Linse, 2003). Gary and colleagues produced micelleplexes with siRNA and poly(ethylene glycol)-poly(n-butyl acrylate)-poly(2-(dimethylamino)ethyl methacrylate) (PEG-PnBA-PDMAEMA), and they proved that due to the coexistence of PEG (PEO) chains in the micelle corona layer, the hydrodynamic thickness of the micelle corona increases with ligation of RNA (Gary *et al.*, 2011).

In the case of PEA 3, the particle size is constant even with the increase in 5 and 10 times more of PEA. Supposedly, an increase in the quantity of PEA could mean an increase of the positive charges, due to the augment of the amino groups. However, the particle size does not suffer significant alterations, probably justified on a poor binding capacity. The decrease in size with an increase in PEA quantity, ratios 5/1 and 10/1, more pronounced in PEA1 and PEA2, is explicated by a better distribution of RNA for the particles, more repulsion and less possibility of agglomeration.

In terms of dispersity, the results show for all PEAs formulations a polydispersion index (PDI) between 0.152 and 0.342, which means a moderate dispersity, but with acceptable values. There also exists a bigger particle dispersity between the N/P ratios in PEA 3, with a significant difference between the N/P ratio 1/1 and 10/1, probably, due to some agglomeration or a more pronounced difference between particle sizes. This data is in accord with the previous results obtained for PEA 3 micelles, which in terms of zeta potential presented a huge standard deviation.

Relatively to zeta potential results, the zeta potential increases with an augment in N/P ratio due to the highest quantity of PEA and with this a highest number of amino groups, positive charges. Comparing these results with the zeta potential results of PEA micelles without small RNA, all conditions presented a decrease in values of zeta potential. This can be explained by the linkage between the negative charge of small RNA, with the positive charge of PEA. The neutralization of the surface charge is more pronounced in PEA 1 and 2 because they present a more relevant decrease in zeta potential values of micelleplexes developed, revealing the highest capacity to interact with the small RNA.

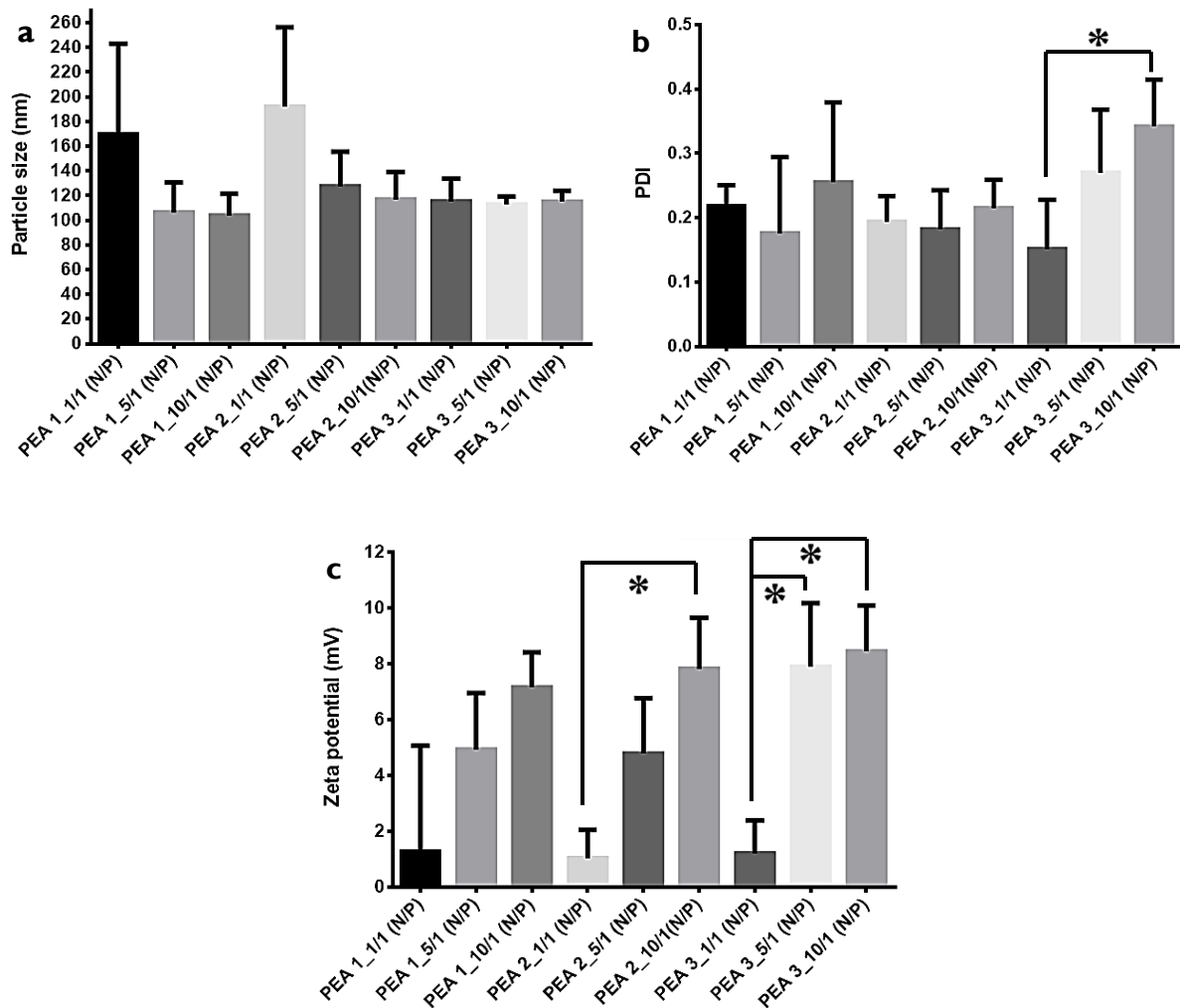


Figure 11 - DLS data of micelleplexes for different PEA and different N/P ratios, in terms of (a) particle size, (b) PDI and (c) zeta potential. (\* $p < 0,05$ )

### 3.3.2.1 Encapsulation efficiency

The encapsulation efficiency was evaluated by an agarose gel assay, represented in figure 12. Thereby, it is possible to observe that only the N/P ratio 1/1, for all the PEAs formulations, was not capable to condense all the small RNA added. Moreover, it is also possible to say that the PEA 3 formulation is the one with less capacity to bond the small RNA, because the appearance of a more intense band for this N/P ratio. These data confirm the anterior results. The remaining N/P ratios, 5/1 and 10/1, for all PEAs formulations, do not present any band, which allows to conclude that small RNA was linked to PEAs. The ratio 1/1, that represents the less quantity of PEA, is unable to condense all small RNA, because less quantity of amino groups is available to bind the small RNA. The values of encapsulation

efficiency were calculated for ratios 1/1, because are the only that presented a band in gel (see table 6).

Confronting all data, the PEA 2 formulation was the one with the better results, due to the less standard deviations, to the presence of a final molar ratio similar to the expected and to present more explicable results.

Table 6 - Data from encapsulation efficiency of different PEAs for ratio 1/1 (N/P).

<b>Encapsulation efficiency</b>	
<b>PEA1_1/1</b>	72%
<b>PEA2_1/1</b>	68%
<b>PEA3_1/1</b>	58%

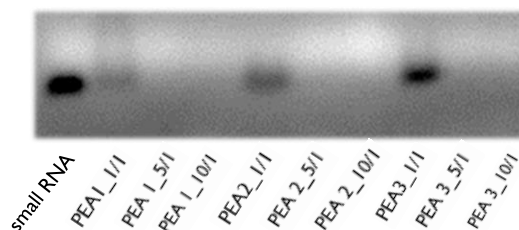


Figure 12 - Representation of an agarose gel retardation assay with the different PEAs and different N/P ratios.

### 3.3.3 Micelleplexes with miR-145 mimic

After the selection of the best PEA formulation, it was performed a physical characterization using the same studies realized previously, however, in this case, complexes were formed through the condensation of miR-145 mimic with the PEA formulation chosen, at the N/P ratios 5/1 and 10/1. The use of only two N/P ratios is related to the zeta potential of micelleplexes. A net positive surface charge allows a higher interaction with the negatively charged cell membrane relative to molecules with a negative charge or neutral molecules (Fröhlich, 2012). Because of the N/P ratio 1/1 presents particles with low zeta potential, close to neutral, the choice went to the other two ratios.

The results of particle size, zeta potential, and PDI are represented below, in figure 13. In terms of size, the results point to a particle size, for both ratios, around 200 nm. The bigger particles were obtained with the higher N/P ration but with no significant differences. Similar to previous results, these particles presented a particle size superior to 200nm. However, the miR-145 mimic used has a molecular weight of, approximately, 14715 Daltons, which is much smaller than the previously used. In this particular case, due to the smaller size of miR-145 mimic, it is possible the binding of various miR-145 mimics to particles, which translate an augment in particle size.

The values of dispersity, reveal particles with a PDI below 0.4, which are acceptable values, assuming a moderate dispersity.

The results obtained for zeta potential show that the values obtained are similar to the results determined to the complexes containing small RNA. The N/P ratio 10/1 presents particles with higher zeta potential, like it was expected.

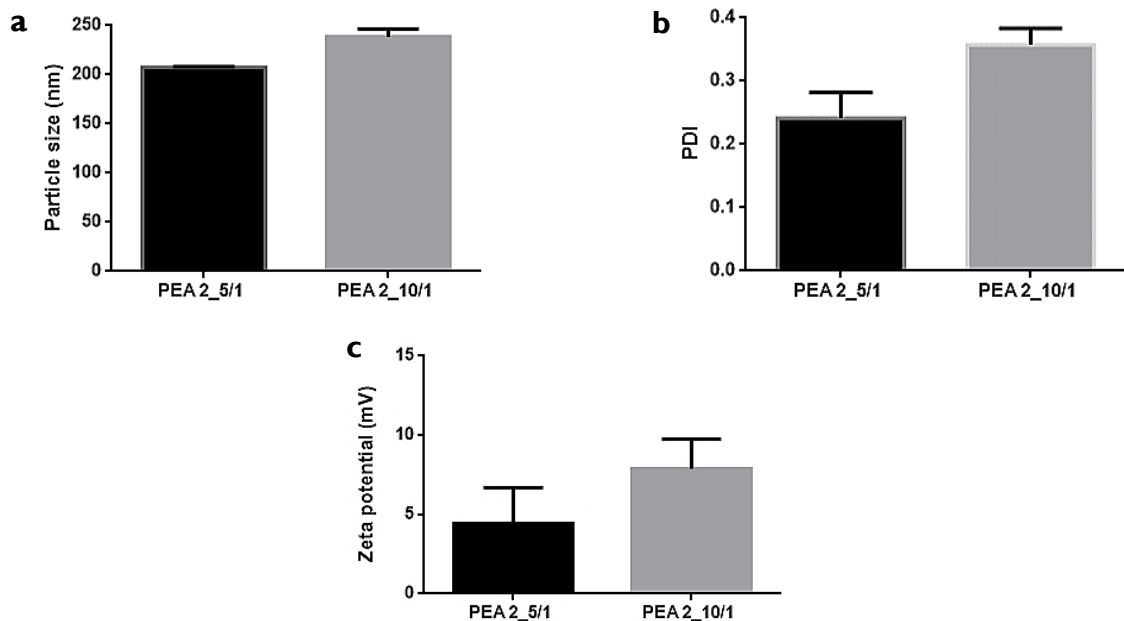


Figure 13 - DLS data of micelleplexes with miR-145 mimic for PEA 2 at ratios 5/1 and 10/1 (N/P), in terms of (a) particle size, (b) PDI and (c) zeta potential.

### 3.3.3.1 Encapsulation efficiency

The binding affinity of miRNA-145 to PEA micelle complexes was also evaluated for both two N/P ratios 5/1 and 10/1. The gel image is represented in figure 14. In the gel image is possible perceive that only appears the band for miR-145 mimic. In both ratios 5/1 and 10/1, similarity to anterior results, does not appears any band, which means that both formulations are able to bind the miR-145 mimic.

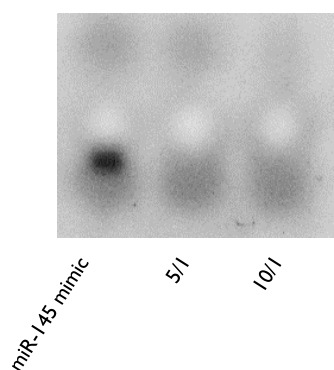


Figure 14 - Representation of an agarose gel retardation assay with miR-145 mimic and two N/P ratios 5/1 and 10/1.

### 3.3.4 Morphology characterization

Samples of PEA micelles and micelleplexes with miR-145 mimic were analyzed by TEM, in order to observe the morphology of both, micelles and micelleplexes. The obtained TEM images are represented in figure 15. Thus, it is observed that the micelles produced with PEA 2 present a well-defined spherical structure, a darker core and a clear shell, which may correspond to PEI chains due to the hydrophilic properties of PEI (figure 15a) (Shen *et al.*, 2014).

Relatively to micelleplexes, figure 15b, it is possible to observe that the structure changes a little bit, with a more irregular spherical shape. The reason for the alteration in the nanoparticle appearance is the miRNA linkage. The miRNA interacts with PEI that is in the shell of the micelle, involving the micelle and altering your spherical shape. In terms of particle size, in micelles, it is possible to verify a little dispersion with large and small particles, but being present particles with sizes that correspond to the obtained by DLS. In this way, it is necessary taking into account that the sample used is smaller than the used for DLS analysis. The micelleplexes presented good homogeneity but with smaller sizes in TEM image comparing to DLS results. These results are probably associated with an artefact result of TEM processing which required the samples to be dried, affecting the final particle size (Wang *et al.*, 2016).

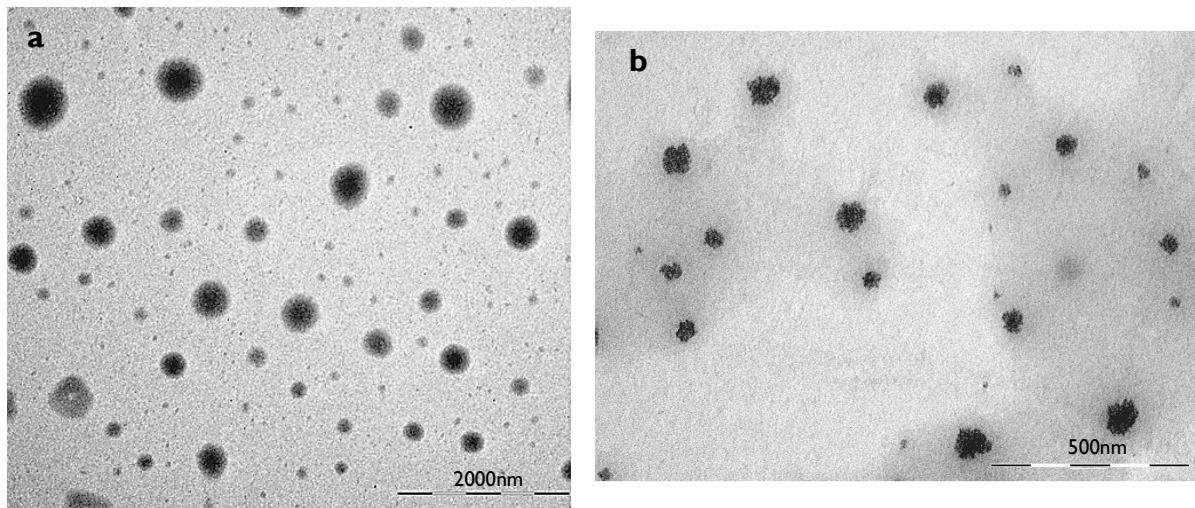


Figure 15 - TEM images of PEA 2 micelles (a), and of micelleplexes with ratio 10/1 (N/P) at a concentration of 50nM of miR-145 mimic (b).

### 3.4 Binding and uptake assay

The binding and uptake assay was realized at 37°C and 4°C because at 4°C the cell metabolism is inhibited and only is evaluated the binding of micelleplexes. On the other hand, at 37°C is possible to evaluate the uptake by the cell membrane.

The results are represented in Figure 16. Figure 16a represents the results obtained for the binding assay, while figure 16b shows the results from the uptake of micelleplexes by the target cells. The values are expressed in RFU, which means relative fluorescence units. The 10nM and 50nM correspond to the concentration used for miR-145 mimic.

It is possible to observe that for both studies, binding and uptake, the N/P ratio 10/1 at a concentration of 10 nM has similar values to the N/P ratio 5/1 at a concentration of 10 nM, which is not expected. The N/P ratio 10/1, with a concentration of 10nM, should be presented the highest values comparing to N/P ratio 5/1, at a concentration of 10 nM, because it should exist a bigger quantity of PEA micelles, which should mean a higher quantity of micelleplexes to bond the cell membrane and, consequently, to be internalized.

For the other two N/P ratios, where is used 50 nM of miR-145 mimic, it was observed an increase of the fluorescence, which means the highest internalization of micelleplexes. This result is expected due to the fact that is used a bigger amount of PEA micelles.

Confronting all the results, it is possible to conclude that micelleplexes are capable of bond and to be internalized by the cell membrane.

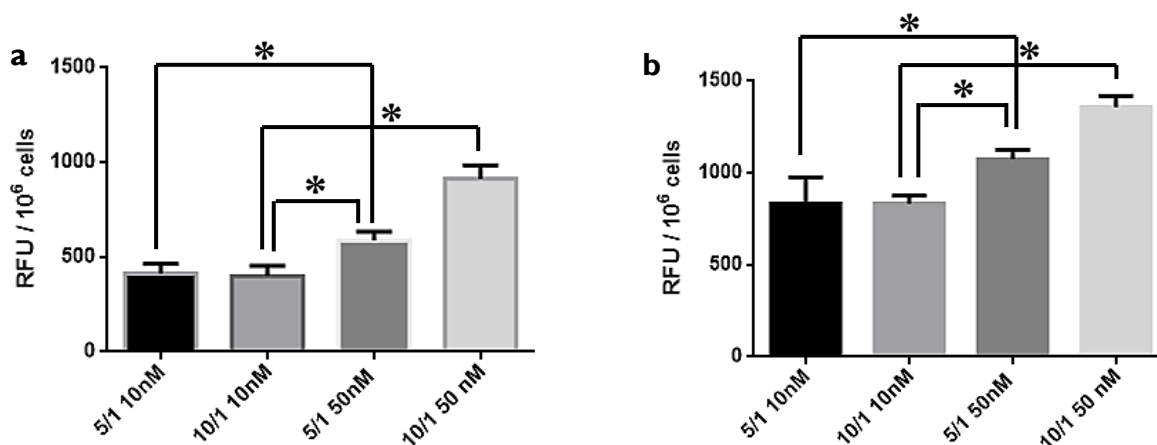


Figure 16 - Results from binding (a), and internalization (b), of micelleplexes at different ratios and concentrations, expressed in relative fluorescence units (RFU). The ratios 5/1 and 10/1 are related to N/P ratio and 10nM and 50nM refer the concentration of miR-145 mimic. (\*p < 0.05)

### 3.5 Cell death assessment

#### 3.5.1 Cell viability

The cytotoxicity for all the studied polymers was analysed and compared. All the PEAs, the Pluronic L64 and PEI were added to cell lines at a final concentration of 5, 10, 20 and 40  $\mu\text{g}/\text{mL}$  and the results for % of viability are represented in figure 17. In figure 17a is represented the results of different concentrations of Pluronic L64 and PEI and in figure 17b the results of the diverse concentrations of all PEAs.

Confronting the results, it is possible to conclude that both Pluronic L64 and all PEAs do not present cytotoxicity in COS-7 cell line until the maximum concentration of 40  $\mu\text{g}/\text{mL}$ . The PEI presented some cytotoxicity at maximum concentration of 40  $\mu\text{g}/\text{mL}$ . It is expected the cytotoxicity of PEI, because free PEI interacts with cellular components inhibiting normal cellular processes (Lv *et al.*, 2006). Also, in another study, it was demonstrated some cytotoxicity of a smaller branched PEI of 1200Daltons with concentrations above 10  $\mu\text{g}/\text{mL}$  (Wang *et al.*, 2016).

The major increase of living cells in PEA, is associated to Pluronic L64 because both values are similar. The explanation is in the fact that some poloxamers, majority poloxamers with high HLB, have stronger shear protective effect on cells (Chang *et al.*, 2017). Independent of L64 does not present a higher HLB, it can have these effects at the used concentrations.

Comparing all results, it is possible to conclude that the conjugation between Pluronic L64 and PEI forms a final product, PEA, noncytotoxic. This conjugation reduces the cytotoxicity associated with PEI.

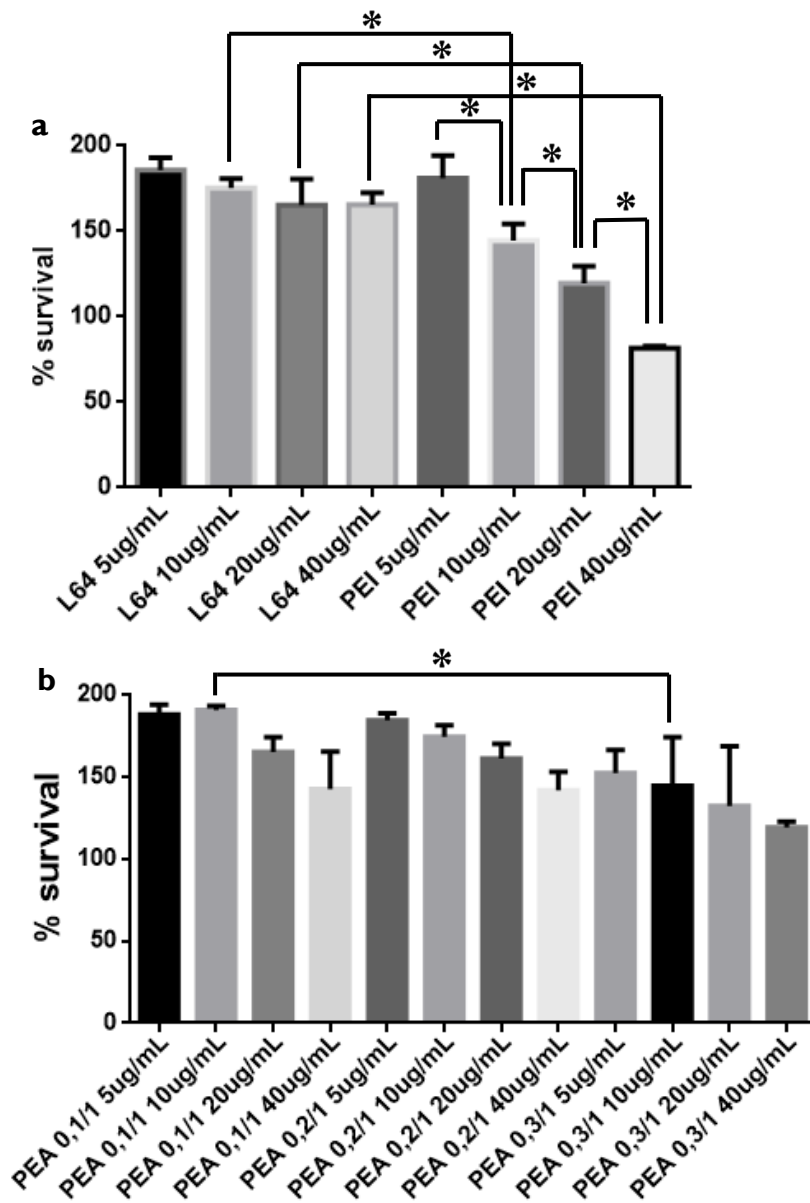


Figure 17 - Cell viability of different polymers, Pluronic L64 and PEI (a), and PEA 1, 2 and 3 (b) at concentrations of 5, 10, 20 and 40µg/mL. (\*p < 0.05)

In order to verify if the micelleplexes were capable of transport the miR-145 mimic to MG-63 cells cytoplasm and kill the osteosarcoma cells a cytotoxicity assay, figure 18, was realized. The expression “NT” in figure 18 means that in these conditions were used a miR non-target, which corresponds to a negative control.

The results of cytotoxicity are illustrated in figure 18, which are divided in two graphs that correspond to cytotoxicity at 24 hours and 48 hours after transfection. It is possible to observe that at 24 hours, figure 18a, all conditions present similar values, with no significant

differences. However, all the samples tested present little cytotoxicity with values between 82% and 88% of cell viability. Comparing with cell viability at 48 hours, figure 18b, it is possible to observe that only two conditions, where are used the highest ratio 10/1 and highest concentration of miR-145 mimic and miR non-target, 50nM, presented a decrease in cell viability.

In both assays, the condition that revealed the highest cytotoxicity was the ratio 10/1 with 50nM of miR-145 mimic. An increased in concentration of miR-145 mimic with a highest concentration of PEA 2 tends to a higher osteosarcoma cell death. In another study where it was used the miR-145 mimic, it was also proved that miR145-mimic at 50nM is able to suppress cell proliferation in MG-63 cell line by targeting the friend leukemia virus integration 1 gene (FLI-1) (Wu *et al.*, 2016).

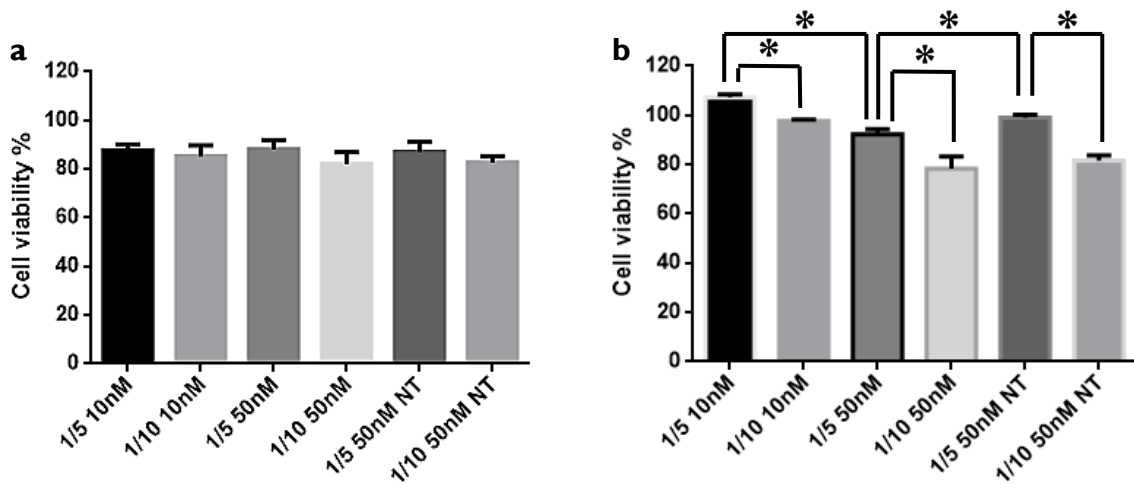


Figure 18 - Cell viability of micelleplexes with different ratios and concentrations at 24hours (a) and 48hours (b) after transfection. The ratios 5/1 and 10/1 are associated with N/P ratio and the expression “NT” refers to the use of miR non-target. 10nM and 50nM refer the concentration of miR-145 mimic or, when applicable, the miR non-target. (\*p < 0.05)

### 3.5.2 Flow cytometry

A flow cytometry assay, figure 19, was performed in order to know the dead type, necrosis or apoptosis. The term “non-targeted” in figure 19a means that in these conditions was used miR non-target. Regarding this, the results of flow cytometry were divided into two parts: a graph, figure 19a which contempts all the information about the dead type of each condition; and 3 images of flow cytometry, with the relevant conditions, figures 19b, 19c, and 19d.

In figure 19a, the graph shows that, for all conditions, the huge part of cells is in late apoptosis/secondary necrosis, including the control condition. This can be explained by the treatment that is necessary to perform for cell detachment which can also kill the untreated

cells (control). However, it is also possible to observe that the condition with the N/P ratio 10/1, with a concentration of 50nM, leads to a higher initial apoptosis and late apoptosis/secondary necrosis. This can also be seen in figure 19d, which illustrates the major quantity of cells in upper right quadrant, related to late apoptosis/secondary necrosis, and upper left quadrant, related to initial apoptosis, comparing to the other two conditions, the control, in figure 19b, and the N/P ratio 10/1, at a concentration of 50nM of a non-targeted sequence, in figure 19c.

The results obtained are similar to the observed in the study mentioned, where it is demonstrated that transfection of miR-145 mimic, at a concentration of 50 nM, with Lipofectamine 3000 resulted in values of apoptosis between 20-25% in MG-63 cell line (Wu *et al.*, 2016). However, it is necessary to emphasize that transfection in the study was done for 24 hours and with a top market in transfection, the Lipofectamine.

It is necessary take in account that the maximum concentration of PEA 2 used in COS-7 cell line was of 40µg/mL which corresponds to 1,304µM, an approximately 2.6-fold increase that maximum concentration of PEA 2 used in MG-63 cell line. In COS-7 cell line that concentration does not reveal cytotoxicity and in the assay with micelleplexes some cell death was revealed. In this case, the cytotoxic effect observed in MG-63 cell line was caused by the miR-145 mimic. Independent of the lack of significant differences, it is possible to observe, mainly in results from flow cytometry, that micelleplexes with miR-145 mimic cause the highest cell death.

Basically, micelleplexes were able to disaggregate and to release the miR-145 mimic, because some therapeutic effects were observed in the results. However, the results were not significant, probably due to the less quantity of miR-145 mimic, to an inefficient release of miR-145 from micelleplex or few micelleplexes that can internalize.

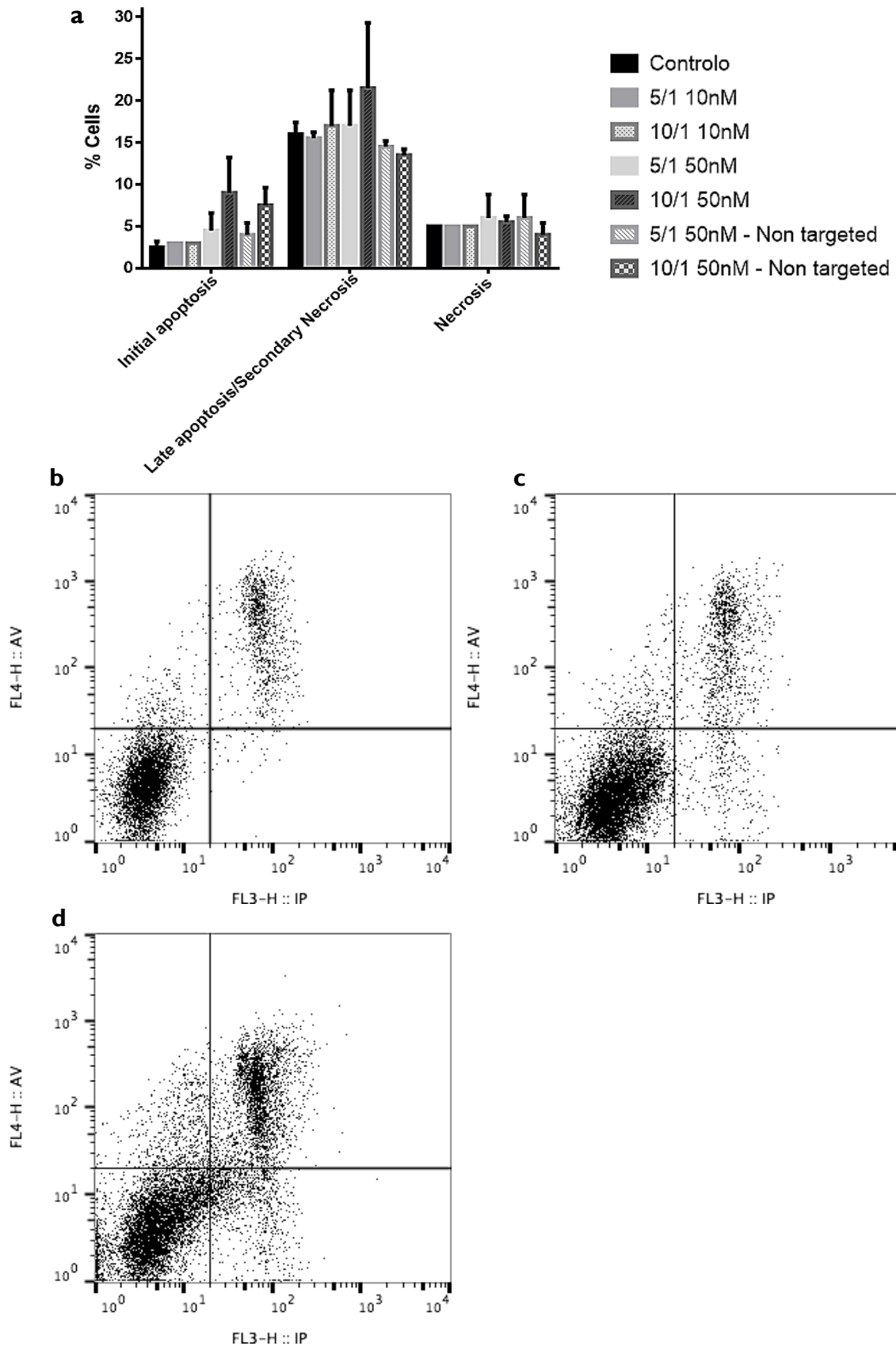


Figure 19 - Flow cytometry results of all conditions (a), and images of flow cytometry of control (b), ratio 10/1 50nM non-targeted, (c) and ratio 10/1 50nM (d). The 5/1 and 10/1 are associated with N/P ratio and the expression “non-targeted” refers to the use of miR non-target. 10nM and 50nM refer the concentration of miR-145 mimic or, when applicable, the miR non-target. The different quadrants in flow cytometry images (b), (c) and (d) means: lower left quadrant – living cells; lower right quadrant – necrotic cells; upper left quadrant – apoptotic cells; upper right quadrant – late apoptotic cells/ secondary necrotic cells.

In order to confirm the results of flow cytometry and to observe the morphology changes caused by the different conditions tested, some smears of samples were performed and analyzed in an optical microscopic. The images of the relevant conditions are represented in figure 20. The control condition, in figure 20a, which represents untreated cells; the N/P ratio 10/1 50nM in figure 20b and 20c representing an apoptotic cell and a necrotic cell, respectively.

It is possible to observe that the untreated cell, figure 20a, does not present a regular form with slight protuberances in the cell membrane. The untreated MG-63 cells presented a stretched form when cultured in monolayer, however, due to the necessary treatments, like cell detachment, the cells alter their structure being more shrunken and rounded, similar to three-dimensional tumor spheroids (Santini *et al.*, 2004).

It is possible to conclude that the micelleplexes produced at an N/P ratio 10/1 with 50nM of miR-145 mimic are, definitively, capable of cause cell apoptosis and necrosis. It is possible to observe in figure 20b the shrinkage of cytoplasm and formations of blebs in the cell membrane, which is indicative of programmed cell death, namely apoptosis. On the other hand, in figure 20c, is only present the cell nucleus due to the burst and breakage of cell membrane caused by cell swelling. These cell characteristics are related to a necrotic cell (Rello-Varona *et al.*, 2015).

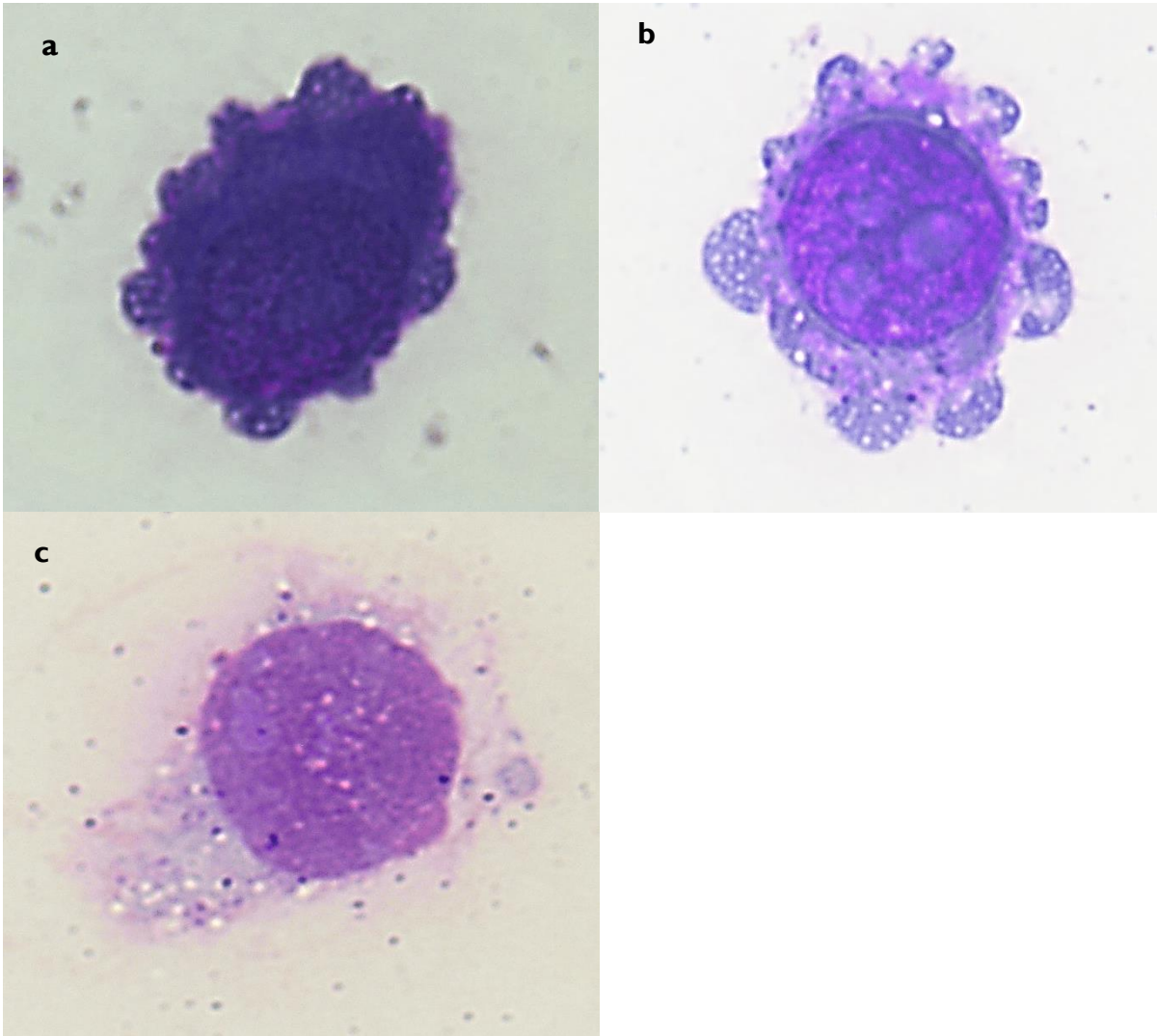


Figure 20 - Optical microscopy images of different conditions tested. Non-treated cells, which represents a normal cell (a), 10/1 (N/P) with 50nM of miR-145mimic, representing an apoptotic cell (b) and same condition, 10/1 (N/P) 50nM of miR-145 mimic, representing a necrotic cell (c). The images were taken at a final magnification of 1000x.

## **4. Conclusion and future perspectives**

In this work, it was demonstrated the possibility to conjugate an amphiphilic block copolymer with the capacity to self-assemble in a micellar structure in an aqueous medium, namely Pluronic L64, to a cationic polymer with high transfection efficiency, namely PEI. Through this conjugation, it was obtained the final product PEA, which has been showing good solubility in water and low cytotoxicity up to concentrations of 40 $\mu$ g/mL. Therefore, this conjugation seems to turn possible the reduction of the cytotoxicity associated to PEI. Despite this, the control of the quantities used in the chemical synthesis of L64 and PEI allows obtaining final products with different molecular weights and characteristics. In this regard, these nanosystems present unique features, such as the ability to escape from a non-specific capture by RES, an EPR effect in places like tumors, a higher stability and a reduced cytotoxicity due to disassembling of micelles in single chains, which is easily excreted.

Thus, the conjugation between these two polymers allowed the production of micellar nanosystems with cationic properties, namely L64-PEI. These micellar nanosystems presented high values of zeta potential, which can mean a higher stability, with size values between 100-200nm and acceptable dispersity. Taking into account these characteristics, the best final product was obtained for the ratio Pluronic L64-PEI 0.2/1 (PEA 2), in which these nanosystems presented a regular spherical shape.

Following this, it was developed micelleplexes through electrostatic interactions between the PEA 2 formulation and miR-145 mimic, at different N/P ratios. These micelleplexes showed a good capacity to bind the miR-145, mainly at higher N/P ratios, and, subsequently, they present the best values for encapsulation efficiency of miR-145 mimic, which can be explained by the increasing amount of PEA used relatively to miR-145 mimic. Besides this, these micelleplexes presented an increase in the particle size relative to PEA micelles alone, which is expected, since the existence of PEO chains in the micelle external layer can promote an increase of the hydrodynamic thickness of the micelle corona when occurs an interaction with miRNA. Apparently, this interaction with the genetic material also induced slightly changes in the micellar shape to a more irregular spherical form. Another important aspect, it was the capacity of these micelleplexes to bind and internalize OS cells, in an efficient way. Furthermore, these complexes demonstrated to be able to cause cell death, limiting the cell growth, being the N/P ratio 10/1 with 50nM of miR-145 mimic who reveals the highest antitumor activity, leading to an apparent programmed cell death (apoptosis). So, it is necessary to take into account that this work shows a promising nanosystem to be applied in a future therapeutic alternative for OS, by using a therapeutic nucleic acid that is able to

reduce the capacity of tumor proliferation, being this effect characteristic of miR-145 mimic in OS cells.

In spite of this, in future studies, it is necessary to repeat some assays to complement this work, such as the increasing N/P ratios, augment of the miRNA concentration and evaluate the degradation of the complexes and the pH influence. Another important aspect is to determine the CMC, which gives more information about micelles stability, through the Wilhelmy plate method or by the optimization of other methods, since in this work it was used two methods, namely DLS data and pyrene probe, and the results obtained were inconclusive.

As aforementioned, micelleplexes have the advantage that can be used for both pharmacotherapy and gene therapy, being possible, in the future, to perform a combined therapy by encapsulating a hydrophobic antitumoral drug, widely used in OS, like doxorubicin, and the therapeutic genetic material miR-145.

## 5. References

AGUILAR, M.Rosa *et al.* - Smart polymers and their applications as biomaterials. Em ASHAMMAKHI, N.; REIS, R.; CHIellini, E. (Eds.) - **Topics in tissue engineering**. v. 3.

AIED, Ahmed *et al.* - Polymer gene delivery: Overcoming the obstacles. **Drug Discovery Today**. ISSN 13596446. 18:21–22 (2013) 1090–1098. doi: 10.1016/j.drudis.2013.06.014.

AKINCHINA, Anna; LINSE, Per - Monte Carlo Simulations of Polyion–Macroion Complexes. 2. Polyion Length and Charge Density Dependence †. **The Journal of Physical Chemistry B**. ISSN 1520-6106. 107:32 (2003) 8011–8021. doi: 10.1021/jp022460f.

ALVAREZ-LORENZO, Carmen *et al.* - Poloxamine-based nanomaterials for drug delivery. **Frontiers in bioscience elite edition**. ISSN 1095-9203. 337:2012 (2012) 303–305. doi: 10.1126/science.1219657.

AMERICAN CANCER SOCIETY - **What Is Osteosarcoma?** [Em linha], atual. 2016. [Consult. 30 jan. 2017]. Disponível em WWW:<URL:<https://www.cancer.org/cancer/osteosarcoma/about/what-is-osteosarcoma.html>>.

BARBULESCU, Denise M.; BURTON, Wayne A.; SALISBURY, Philip A. - Pluronic F-68: an answer for shoot regeneration recalcitrance in microspore-derived *Brassica napus* embryos. **In Vitro Cellular & Developmental Biology - Plant**. ISSN 1054-5476. 47:2 (2011) 282–288. doi: 10.1007/s11627-011-9353-8.

BATRAKOVA, Elena V.; KABANOV, Alexander V. - Pluronic block copolymers: Evolution of drug delivery concept from inert nanocarriers to biological response modifiers. **Journal of Controlled Release**. ISSN 01683659. 130:2 (2008) 98–106. doi: 10.1016/j.jconrel.2008.04.013.

CAGEL, Maximiliano *et al.* - Polymeric mixed micelles as nanomedicines: Achievements and perspectives. **European Journal of Pharmaceutics and Biopharmaceutics**. ISSN 09396411. January (2017). doi: 10.1016/j.ejpb.2016.12.019.

CATALANOTTO, Caterina; COGONI, Carlo; ZARDO, Giuseppe - MicroRNA in Control of Gene Expression: An Overview of Nuclear Functions. **International Journal of Molecular Sciences**. ISSN 1422-0067. 17:10 (2016) 1712. doi: 10.3390/ijms17101712.

CHANG, David *et al.* - Investigation of interfacial properties of pure and mixed poloxamers for surfactant-mediated shear protection of mammalian cells. **Colloids and Surfaces B: Biointerfaces**. ISSN 09277765. 156:2017) 358–365. doi: 10.1016/j.colsurfb.2017.05.040.

CHEN, Bin *et al.* - MicroRNA-145 suppresses osteosarcoma metastasis via Targeting MMP16. **Cellular Physiology and Biochemistry**. ISSN 14219778. 37:6 (2015) 2183–2193. doi: 10.1159/000438575.

CHEN, Jianlin *et al.* - Increase in transgene expression by pluronic L64-mediated endosomal/lysosomal escape through its membrane-disturbing action. **ACS Applied Materials and Interfaces**. ISSN 19448252. 7:13 (2015) 7282–7293. doi: 10.1021/acsami.5b00486.

CHIAPPETTA, Diego A.; SOSNIK, Alejandro - Poly(ethylene oxide)-poly(propylene oxide) block copolymer micelles as drug delivery agents: Improved hydrosolubility, stability and bioavailability of drugs. **European Journal of Pharmaceutics and Biopharmaceutics**. ISSN 09396411. 66:3 (2007) 303–317. doi: 10.1016/j.ejpb.2007.03.022.

CHITKARA, Deepak; SINGH, Saurabh; MITTAL, Anupama - Nanocarrier-based co-delivery of small molecules and siRNA/miRNA for treatment of cancer. **Therapeutic Delivery**. ISSN 2041-5990. 7:4 (2016) 245–255. doi: 10.4155/tde-2015-0003.

CLIMA, Lilia *et al.* - Experimental design, modeling and optimization of polyplex formation between DNA oligonucleotides and branched polyethylenimine. **Org. Biomol. Chem.** ISSN 1477-0520. 13:36 (2015) 9445–9456. doi: 10.1039/C5OB01189B.

COLLINS, Mary; THRASHER, Adrian - Gene therapy: progress and predictions. **Proc R Soc B**. ISSN 0962-8452. 282:1821 (2015) 20143003. doi: 10.1098/rspb.2014.3003.

CUI, Shi Yun; WANG, Rui; CHEN, Long Bang - MicroRNA-145: A potent tumour suppressor that regulates multiple cellular pathways. **Journal of Cellular and Molecular Medicine**. ISSN 15821838. 18:10 (2014) 1913–1926. doi: 10.1111/jcmm.12358.

D'ERRICO, Gerardino; PADUANO, Luigi; KHAN, Ali - Temperature and concentration effects on supramolecular aggregation and phase behavior for poly(propylene oxide)-b-poly(ethylene oxide)- b-poly(propylene oxide) copolymers of different composition in aqueous mixtures, I. **Journal of Colloid and Interface Science**. ISSN 00219797. 279:2 (2004) 379–390. doi: 10.1016/j.jcis.2004.06.063.

DAS, Ani V; PILLAI, Radhakrishna M. - Implications of miR cluster 143/145 as universal anti-oncomiRs and their dysregulation during tumorigenesis. **Cancer cell international**. ISSN 1475-2867. 15:2015) 92. doi: 10.1186/s12935-015-0247-4.

DURFEE, Ryan A.; MOHAMMED, Maryam; LUU, Hue H. - Review of Osteosarcoma and Current Management. **Rheumatology and therapy**. ISSN 2198-6576. 3:2 (2016) 221–243. doi: 10.1007/s40744-016-0046-y.

ESTEVEZ, Remelisa *et al.* - Determination of Aqueous Surfactant Solution Surface Tensions with a Surface Tensiometer. **Beyond: Undergraduate Research Journal**. 1:1 (2016).

FAN, Lei *et al.* - MicroRNA-145 targets vascular endothelial growth factor and inhibits invasion and metastasis of osteosarcoma cells. **Acta Biochim Sin.** 44:5 (2012) 407–414. doi: 10.1093/abbs/gms019.Advance.

FAN, Wei *et al.* - Degradable gene delivery systems based on Pluronic-modified low-molecular-weight polyethylenimine: Preparation, characterization, intracellular trafficking, and cellular distribution. **International Journal of Nanomedicine**. ISSN 11769114. 7:2012) 1127–1138. doi: 10.2147/IJN.S27117.

FLETCHER, C. D.M., BRIDGE, J.A., HOGENDOORN, P., MERTENS, F. - WHO Classification of Tumours, Volume 5. Em **WHO Classification of tumors of soft tissue and bone**.

GARY, Dana J. *et al.* - Influence of Nano-Carrier Architecture on in Vitro siRNA Delivery Performance and in Vivo Biodistribution: Polyplexes vs Micelleplexes. **ACS Nano**. ISSN 1936-0851. 5:5 (2011) 3493–3505. doi: 10.1021/nn102540y.

GRAAF, Albert J. DE *et al.* - Looped Structure of Flowerlike Micelles Revealed by 1 H NMR Relaxometry and Light Scattering. **Langmuir**. ISSN 0743-7463. 27:16 (2011) 9843–9848. doi: 10.1021/la2019605.

GUO, Xia; HUANG, Leaf - Recent Advances in Non-viral Vectors for Gene Delivery. **Accounts of Chemical Research**. ISSN 00014842. 45:7 (2013) 971–979. doi: 10.1021/ar200151m.Recent.

HERZBERGER, Jana *et al.* - Polymerization of ethylene oxide, propylene oxide, and other alkylene oxides: Synthesis, novel polymer architectures, and bioconjugation. **Chemical Reviews**. ISSN 15206890. 116:4 (2016) 2170–2243. doi: 10.1021/acs.chemrev.5b00441.

HÖBEL, Sabrina; AIGNER, Achim - Polyethylenimines for siRNA and miRNA delivery in vivo. **Wiley Interdisciplinary Reviews: Nanomedicine and Nanobiotechnology**. ISSN 19395116. 5:5 (2013) 484–501. doi: 10.1002/wnan.1228.

HU, Hao *et al.* - Changes in microRNA expression in the MG-63 osteosarcoma cell line compared with osteoblasts. **Oncology Letters**. ISSN 17921074. 4:5 (2012) 1037–1042. doi: 10.3892/ol.2012.866.

HUANG, Xiangxuan *et al.* - pH-sensitive micelles self-assembled from polymer brush (PAE-g-cholesterol)-b-PEG-b-(PAE-g-cholesterol) for anticancer drug delivery and controlled release. **International Journal of Nanomedicine**. ISSN 1178-2013. Volume 12:2017) 2215–2226. doi: 10.2147/IJN.S130037.

JAFARI, M. *et al.* - Nonviral Approach for Targeted Nucleic Acid Delivery. **Current Medicinal Chemistry**. ISSN 09298673. 19:2 (2012) 197–208. doi: 10.2174/092986712803414141.

JAFARLOU, M. *et al.* - An overview of the history, applications, advantages, disadvantages and prospects of gene therapy. **Journal of biological regulators and homeostatic agents**. ISSN 0393974X. 30:2 (2016) 315–321.

JHAVERI, Aditi M.; TORCHILIN, Vladimir P. - Multifunctional polymeric micelles for delivery of drugs and siRNA. **Frontiers in Pharmacology**. ISSN 1663-9812. 5:April (2014) 1–26. doi: 10.3389/fphar.2014.00077.

Jl, Weidan; SUN, Bin; SU, Changqing - Targeting MicroRNAs in Cancer Gene Therapy. **Genes**. ISSN 2073-4425. 8:1 (2017) 21. doi: 10.3390/genes8010021.

JIN, Lian *et al.* - Current progress in gene delivery technology based on chemical methods and nano-carriers. **Theranostics**. ISSN 18387640. 4:3 (2014) 240–255. doi: 10.7150/thno.6914.

JUNG, Y. W. *et al.* - Pluronic-based core/shell nanoparticles for drug delivery and diagnosis. **Curr Med Chem**. 20:28 (2013) 3488–3499.

KABANOV, A. V; BATRAKOVA, E. V; ALAKHOV, V. Y. - Pluronic (R) block copolymers as novel polymer therapeutics for drug and gene delivery. **Journal of Controlled Release**. ISSN 01683659. 82:2–3 (2002) 189–212. doi: 10.1016/s0168-3659(02)00009-3.

KABANOV, Alexander; ZHU, Jian; ALAKHOV, Valery - Pluronic Block Copolymers for Gene

Delivery. **Advances in Genetics**. ISSN 00652660. 53:5 (2005) 231–261. doi: 10.1016/S0065-2660(05)53009-8.

KELES, Erhan *et al.* - Recent progress in nanomaterials for gene delivery applications. **Biomaterials Science**. ISSN 2047-4830. 4:9 (2016) 1291–1309. doi: 10.1039/C6BM00441E.

KIM, Jayoung *et al.* - Targeted polymeric nanoparticles for cancer gene therapy. **Journal of Drug Targeting**. ISSN 1061-186X. 23:7–8 (2015) 627–641. doi: 10.3109/1061186X.2015.1048519.

KIM, Tae Hee *et al.* - A degradable hyperbranched poly(ester amine) based on poloxamer diacrylate and polyethylenimine as a gene carrier. **Macromolecular Bioscience**. ISSN 16165187. 7:5 (2007) 611–619. doi: 10.1002/mabi.200600245.

KOZLOV, Mikhail Yu *et al.* - Relationship between pluronic block copolymer structure, critical micellization concentration and partitioning coefficients of low molecular mass solutes. **Macromolecules**. ISSN 00249297. 33:9 (2000) 3305–3313. doi: 10.1021/ma991634x.

KUNDU, Zile Singh - Classification, imaging, biopsy and staging of osteosarcoma. **Indian Journal of Orthopaedics**. ISSN 0019-5413. 48:3 (2014) 238–246. doi: 10.4103/0019-5413.132491.

LI, Enqi *et al.* - MiR-145 inhibits osteosarcoma cells proliferation and invasion by targeting ROCK1. **Tumour biology: the journal of the International Society for Oncodevelopmental Biology and Medicine**. ISSN 14230380. 35:8 (2014) 7645–7650. doi: 10.1007/s13277-014-2031-9.

LI, Yimu *et al.* - Folate-modified pluronic-polyethylenimine and cholic acid polyion complex micelles as targeted drug delivery system for paclitaxel. **Journal of Microencapsulation**. ISSN 0265-2048. 31:8 (2014) 805–814. doi: 10.3109/02652048.2014.940010.

LINDSEY, Brock A.; MARKEL, Justin E.; KLEINERMAN, Eugenie S. - Osteosarcoma Overview. **Rheumatology and Therapy**. ISSN 2198-6576. 2016). doi: 10.1007/s40744-016-0050-2.

LUNGU, Claudiu N. *et al.* - Linear and branched PEIs (Polyethylenimines) and their property space. **International Journal of Molecular Sciences**. ISSN 14220067. 17:4 (2016). doi: 10.3390/ijms17040555.

LV, Hongtao *et al.* - Toxicity of cationic lipids and cationic polymers in gene delivery. **Journal**

of **Controlled Release**. ISSN 01683659. 114:1 (2006) 100–109. doi: 10.1016/j.jconrel.2006.04.014.

MARTIN, Jeff W.; SQUIRE, Jeremy A.; ZIELENSKA, Maria - The genetics of osteosarcoma. **Sarcoma**. ISSN 1357714X. 2012:2012). doi: 10.1155/2012/627254.

MATA, J. P. *et al.* - Concentration, temperature, and salt-induced micellization of a triblock copolymer Pluronic L64 in aqueous media. **Journal of Colloid and Interface Science**. ISSN 00219797. 292:2 (2005) 548–556. doi: 10.1016/j.jcis.2005.06.013.

MENDES, José *et al.* - L744,832 and Everolimus Induce Cytotoxic and Cytostatic Effects in Non-Hodgkin Lymphoma Cells. **Pathology & Oncology Research**. ISSN 1219-4956. 22:2 (2016) 301–309. doi: 10.1007/s12253-015-9998-4.

MIAO, Jinglei *et al.* - MicroRNAs in osteosarcoma: Diagnostic and therapeutic aspects. **Tumor Biology**. ISSN 10104283. 34:4 (2013) 2093–2098. doi: 10.1007/s13277-013-0940-7.

MIEN-CHIE HUNG, LEAF HUANG, Ernst Wagner - **Nonviral Vectors for Gene Therapy** [Em linha] Disponível em WWW:<URL:http://www.google.se/books?id=ZdzvU3\_yie4C&dq=Non+viral+systems+for+gene+delivery:+up+to+date&lr=&source=gbs\_navlinks\_s>. ISBN 9780128001486.

MOHR, Andreas *et al.* - A New Pyrene-Based Fluorescent Probe for the Determination of Critical Micelle Concentrations. **The Journal of Physical Chemistry B**. ISSN 1520-6106. 111:45 (2007) 12985–12992. doi: 10.1021/jp0731497.

MOKHTARZADEH, Ahad *et al.* - Biodegradable nano-polymers as delivery vehicles for therapeutic small non-coding ribonucleic acids. **Journal of Controlled Release**. ISSN 18734995. 245:2017) 116–126. doi: 10.1016/j.jconrel.2016.11.017.

NASCIMENTO, Débora F. DO *et al.* - Microfluidic Fabrication of Pluronic Vesicles with Controlled Permeability. **Langmuir**. ISSN 0743-7463. 32:21 (2016) 5350–5355. doi: 10.1021/acs.langmuir.6b01399.

NAYEROSSADAT, Nouri; ALI, PalizbanAbas; MAEDEH, Talebi - Viral and nonviral delivery systems for gene delivery. **Advanced Biomedical Research**. ISSN 2277-9175. 1:1 (2012) 27. doi: 10.4103/2277-9175.98152.

OBA, Makoto - Study on development of polymeric micellar gene carrier and evaluation of its

functionality. **Biological & pharmaceutical bulletin**. ISSN 1347-5215. 36:7 (2013) 1045–51. doi: 10.5681/bi.2013.020.

OHNO, Sayaka; ISHIHARA, Kazuhiko; YUSA, Shin Ichi - Formation of Polyion Complex (PIC) Micelles and Vesicles with Anionic pH-Responsive Unimer Micelles and Cationic Diblock Copolymers in Water. **Langmuir**. ISSN 15205827. 32:16 (2016) 3945–3953. doi: 10.1021/acs.langmuir.6b00637.

PEREIRA, Patrícia *et al.* - Smart micelleplexes as a new therapeutic approach for RNA delivery. **Expert Opinion on Drug Delivery**. ISSN 1742-5247. 14:3 (2017) 353–371. doi: 10.1080/17425247.2016.1214567.

PRHASHANNA, Ammu; KHAN, Saif A.; CHEN, Shing Bor - Co-micellization behavior in poloxamers: Dissipative particle dynamics study. **Journal of Physical Chemistry B**. ISSN 15205207. 119:2 (2015) 572–582. doi: 10.1021/jp509237r.

RAMPERSAD, Sephra N. - Multiple Applications of Alamar Blue as an Indicator of Metabolic Function and Cellular Health in Cell Viability Bioassays. **Sensors**. ISSN 1424-8220. 12:12 (2012) 12347–12360. doi: 10.3390/s120912347.

RIZIS, Georgios; VEN, Theo G. M. VAN DE; EISENBERG, Adi - «Raft» Formation By Two-Dimensional Self-Assembly of Block Copolymer Rod Micelles in Aqueous Solution. **Angewandte Chemie - International Edition**. ISSN 15213773. 53:34 (2014) 9000–9003. doi: 10.1002/anie.201404089.

ROQUES, Caroline *et al.* - Parameters affecting organization and transfection efficiency of amphiphilic copolymers/DNA carriers. **Journal of Controlled Release**. ISSN 01683659. 138:1 (2009) 71–77. doi: 10.1016/j.jconrel.2009.04.030.

SERRA, M.; HATTINGER, C. M. - The pharmacogenomics of osteosarcoma. ISSN 1470-269X. April (2016) 1–10. doi: 10.1038/tpj.2016.45.

SIMÕES, Susana M. N. *et al.* - Polymeric micelles for oral drug administration enabling locoregional and systemic treatments. **Expert opinion on drug delivery**. ISSN 1744-7593. 12:2 (2015) 297–318. doi: 10.1517/17425247.2015.960841.

SINGH-JOY, Subhashni D.; MCLAIN, Valerie C. - Safety Assessment of Poloxamers 101, 105, 108, 122, 123, 124, 181, 182, 183, 184, 185, 188, 212, 215, 217, 231, 234, 235, 237, 238, 282, 284, 288, 331, 333, 334, 335, 338, 401, 402, 403, and 407, Poloxamer 105 Benzoate, and

Poloxamer 182 Dibenzoate as Use. **International Journal of Toxicology**. ISSN 1091-5818. 27:2\_suppl (2008) 93–128. doi: 10.1080/10915810802244595.

SUNOQROT, Suhair *et al.* - Kinetically controlled cellular interactions of polymer-polymer and polymer-liposome nanohybrid systems. **Bioconjugate Chemistry**. ISSN 10431802. 22:3 (2011) 466–474. doi: 10.1021/bc100484t.

TAVANO, Lorena *et al.* - Spontaneous temperature-sensitive Pluronic ® based niosomes: Triggered drug release using mild hyperthermia. **International Journal of Pharmaceutics**. ISSN 03785173. 511:2 (2016) 703–708. doi: 10.1016/j.ijpharm.2016.07.064.

TOMASELLI, Sara *et al.* - ADAR enzyme and miRNA story: A nucleotide that can make the difference. **International Journal of Molecular Sciences**. ISSN 16616596. 14:11 (2013) 22796–22816. doi: 10.3390/ijms141122796.

TOPEL, Önder *et al.* - Determination of critical micelle concentration of polybutadiene-block-poly(ethyleneoxide) diblock copolymer by fluorescence spectroscopy and dynamic light scattering. **Journal of Molecular Liquids**. ISSN 01677322. 177:January (2013) 40–43. doi: 10.1016/j.molliq.2012.10.013.

TORCELLO-GÓMEZ, Amelia *et al.* - Block copolymers at interfaces: Interactions with physiological media. **Advances in Colloid and Interface Science**. ISSN 00018686. 206:2014) 414–427. doi: 10.1016/j.cis.2013.10.027.

TRIVEDI, Ruchit; KOMPELLA, Uday B. - Nanomicellar formulations for sustained drug delivery: strategies and underlying principles. **Nanomedicine (London, England)**. ISSN 1748-6963. 5:3 (2010) 485–505. doi: 10.2217/nnm.10.10.

VENKATARAMAN, Shrinivas *et al.* - The effects of polymeric nanostructure shape on drug delivery. **Advanced Drug Delivery Reviews**. ISSN 0169409X. 63:14–15 (2011) 1228–1246. doi: 10.1016/j.addr.2011.06.016.

WAN, Xin *et al.* - ROCK1, a novel target of miR-145, promotes glioma cell invasion. **Molecular Medicine Reports**. ISSN 17913004. 9:5 (2014) 1877–1882. doi: 10.3892/mmr.2014.1982.

WANG, M. *et al.* - Poly(ester amine) constructed from polyethylenimine and pluronic for gene delivery in vitro and in vivo. **Drug Deliv**. ISSN 15210464. 2016) 1–10. doi: 10.3109/10717544.2016.1162877.

WANG, Weiwei *et al.* - Engineering biodegradable micelles of polyethylenimine-based amphiphilic block copolymers for efficient DNA and siRNA delivery. **Journal of Controlled Release**. ISSN 18734995. 242:2016) 71–79. doi: 10.1016/j.jconrel.2016.08.004.

WINTER, Julia *et al.* - Many roads to maturity: microRNA biogenesis pathways and their regulation. **Nature cell biology**. ISSN 1465-7392. 11:3 (2009) 228–234. doi: 10.1038/ncb0309-228.

WU, Panfeng *et al.* - miR-145 promotes osteosarcoma growth by reducing expression of the transcription factor friend leukemia virus integration 1. **Oncotarget**. ISSN 1949-2553. 7:27 (2016) 42241–42251. doi: 10.18632/oncotarget.9948.

XIONG, Xiao Bing *et al.* - Engineering of amphiphilic block copolymers for polymeric micellar drug and gene delivery. **Journal of Controlled Release**. ISSN 01683659. 155:2 (2011) 248–261. doi: 10.1016/j.jconrel.2011.04.028.

YIN, Hao *et al.* - Non-viral vectors for gene-based therapy. **Nat Rev Genet**. ISSN 1471-0056. 15:8 (2014) 541–555. doi: 10.1038/nrg3763.

YOKOYAMA, Masayuki - Polymeric micelles as drug carriers: their lights and shadows. **J Drug Target**. ISSN 1061-186X. 22:7 (2014) 576–583. doi: 10.3109/1061186X.2014.934688.

ZHANG, Yu *et al.* - Reducible Micelleplexes are Stable Systems for Anti-miRNA Delivery in Cerebrospinal Fluid. **Molecular Pharmaceutics**. ISSN 15438392. 13:6 (2016) 1791–1799. doi: 10.1021/acs.molpharmaceut.5b00933.